

BELLCOMM, INC.

955 L'ENFANT PLAZA NORTH, S.W., WASHINGTON, D.C. 20024

COVER SHEET FOR TECHNICAL MEMORANDUM

TITLE- The Navigation System of the
Lunar Roving Vehicle

TM- 70-2014-8

FILING CASE NO(S)- 310

DATE- December 11, 1970

FILING SUBJECT(S)
(ASSIGNED BY AUTHOR(S))- Navigation, LRV

AUTHOR(S)- W. G. Heffron
F. LaPiana

ABSTRACT

The need for the navigation system of the Lunar Roving Vehicle has been evaluated, comparing it with navigation by lunar landmarks and prominent features, and with the ability of the crew to see the Lunar Module at reasonable distances. It is concluded that the navigation system is only a convenience item, not mandatory, and that mission rules should not require the system to be operable either to begin or continue a sortie.

Considered as a convenience item, moderate accuracy requirements are suggested which can be achieved by the equipment being developed and with little inconvenience to the crew. The method of operation and sources of error for the system are analyzed and discussed, and accurate nomographs useful in aligning the directional gyroscope are presented.

DISTRIBUTION

COMPLETE MEMORANDUM TO

CORRESPONDENCE FILES:

OFFICIAL FILE COPY

plus one white copy for each
additional case referenced

TECHNICAL LIBRARY (4)

NASA Headquarters

R. S. Diller/MAT
J. K. Holcomb/MAO
C. M. Lee/MA
A. S. Lyman/MR
B. Milwitzky/MA
W. E. Stoney/MA

Manned Spacecraft Center

J. H. Cooper/FC9
C. M. Duke, Jr./CB
J. B. Irwin/CB
R. H. Kohrs/PD7
G. S. Lunney/FC
J. A. McDivitt/PA
D. B. Pendley/PA
S. Ritchee/SM
J. E. Saultz/FC9
D. R. Scott/CB
J. R. Sevier/PD4
D. K. Slayton/CA
J. L. Smothermon/CF2
H. W. Tindall/FA
J. W. Young/CB

Marshall Space Flight Center

J. D. Alter/PM-SAT-LRV
W. A. Armistead/PM-SAT-LRV
J. A. Belew/PM-SAT-LRV
P. H. Broussard, Jr./S&E-ASTR-GC
S. F. Morea/PM-SAT-LRV
J. M. Sisson/PM-SAT-LRV
F. W. Wagon/PD-AP

Bell Telephone Laboratories, Inc.

D. P. Ling/WH

COMPLETE MEMORANDUM TO

Boeing Company

R. W. Ekis
R. Goodstein
W. Lerchenmueller
L. J. McMurtry
R. M. O'Brien

Bellcomm, Inc.

D. R. Anselmo
I. Y. Bar-Itzhack
P. Benjamin
A. P. Boysen, Jr.
J. O. Cappellari, Jr.
D. A. De Graaf
F. El-Baz
D. R. Hagner
N. W. Hinners
T. B. Hoekstra
M. Liwshitz
J. A. Llewellyn
K. E. Martersteck
J. Z. Menard
J. J. O'Connor
P. F. Sennewald
R. V. Sperry
J. W. Timko
R. L. Wagner
Department 1024 Files

Abstract Only to

NASA Headquarters

R. A. Petrone/MA

Bellcomm, Inc.

J. P. Downs
I. M. Ross
M. P. Wilson

TABLE OF CONTENTS

- 1.0 INTRODUCTION
- 2.0 NEED FOR THE LRV NAVIGATION SYSTEM
- 3.0 FUNCTIONAL DESCRIPTION OF THE NAVIGATION SYSTEM
- 4.0 WHEEL PULSE ACCURACY EFFECTS
- 5.0 GYRO ALIGNMENT ACCURACY EFFECTS
- 6.0 GYRO ALIGNMENT DETERMINATION TECHNIQUES
 - 6.1 The Sun Shadow Device
 - 6.2 Sun Azimuth and Elevation
 - 6.3 Sun Shadow Device Nomographs
 - 6.4 Directional Gyro Angle Nomograph
 - 6.5 Effects of Errors
- 7.0 SUMMARY AND CONCLUSIONS
- 8.0 ACKNOWLEDGMENTS
- 9.0 REFERENCES

SUBJECT: The Navigation System of the Lunar
Roving Vehicle - Case 310

DATE: December 11, 1970

FROM: W. G. Heffron
F. LaPiana

TM-70-2014-8

TECHNICAL MEMORANDUM

1.0 INTRODUCTION

This memorandum is concerned with the navigation system of the Lunar Roving Vehicle (LRV). Planned for use in Apollo missions 15-17, the LRV is used to extend the area around the Lunar Module which can be investigated. The maximum distance the LRV can go from the LM is restricted to 9.5 KM although the LRV has enough battery power to go a total of some 70 KM in sortie distance. This is typically divided into three separate sorties, with rest periods in between, given a total lunar surface stay time of 66 hours. Figure 1 shows preliminary traverses planned for Apollo 15, landing at Hadley-Apennines, and illustrates how the LRV permits sampling material from both the edge of the rille and the foot of the mountains.

The navigation system has two major uses. One is to locate the LRV (with respect to the LM) when specific scientific activity occurs, the other is to show the direction and distance to return to the LM. To do this, it uses a directional gyroscope to resolve wheel rotations into North-South and East-West distance components, and manipulates these to display range and bearing from the LRV to the LM. Navigation system accuracy is reduced by errors in effective wheel size, by wheel slip and by directional gyro azimuth errors. The next section considers what system accuracy is required, in particular considering navigation purely by landmark recognition and by actually seeing the LM. We conclude that the system is not mandatory for a sortie, that it is chiefly a convenience item and should be treated as such. Its accuracy requirements are therefore moderate, not stringent.

Later sections discuss how the system works, evaluate the effects of wheel size and slip and of directional gyro

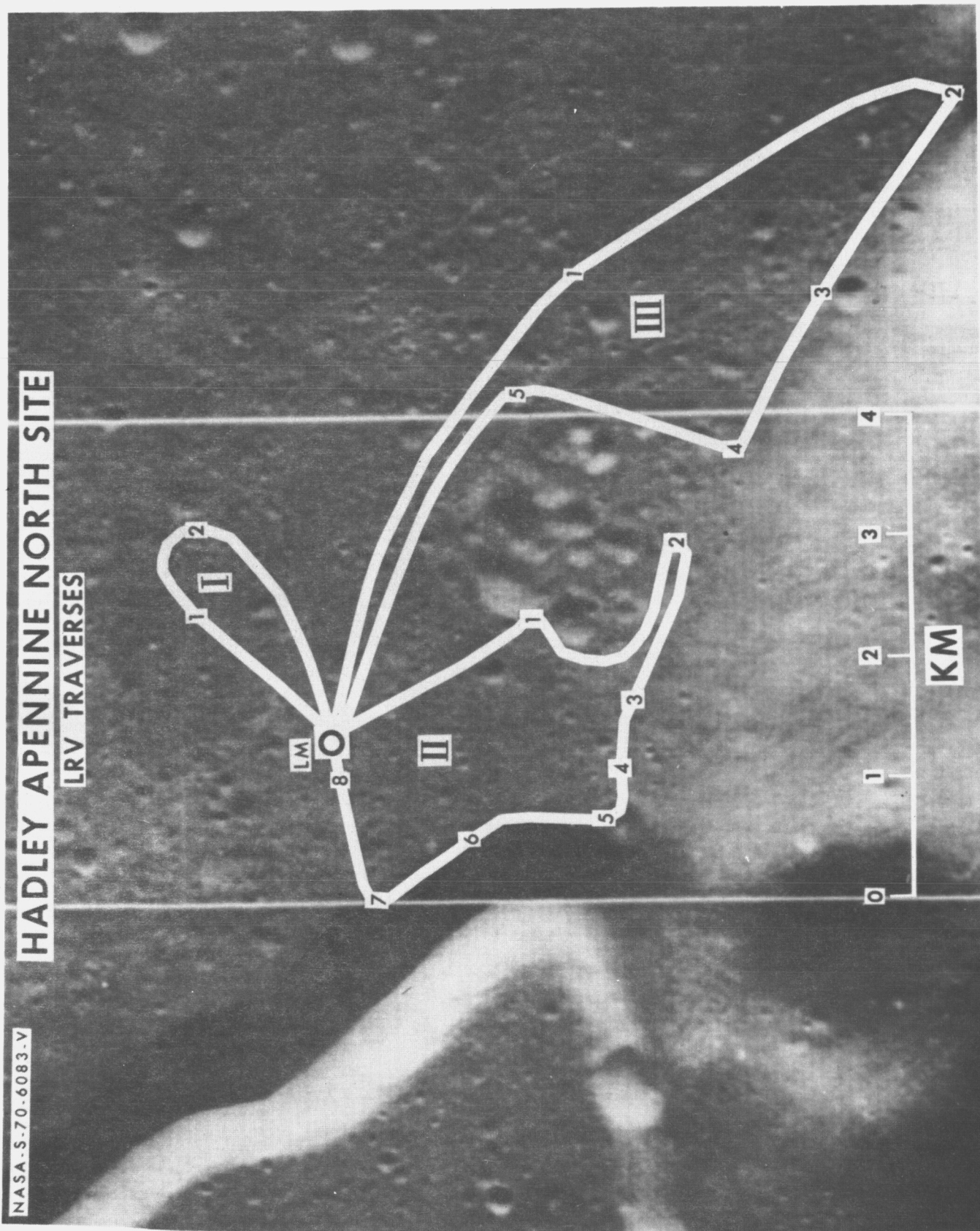


FIGURE 1

accuracy, analyze the Sun Shadow Device used to align the gyro, and present nomographs useful for such purposes. It appears that the system can be helpful to the crew without requiring significant attention by them.

2.0 NEED FOR THE LRV NAVIGATION SYSTEM

The trend in Apollo missions is toward landings in rougher terrain. Such areas are of greater interest scientifically, especially in that the mare areas have already been visited. Figures 1, 2, and 3 show the Hadley-Apennines area to be visited on Apollo 15, and the Copernicus crater, and the Marius Hills area, candidates for later Apollo missions.

A factor in choosing sites is the availability of easily identifiable landmarks. The rille at Hadley, the peaks in Copernicus, and the hills themselves at Marius help the LM Commander assess the LM descent trajectory in guiding it to a "pinpoint" landing at the desired site.

A requirement for selection of a site is that good photography of the area must be available, first to assist in determining if the area is safe for landing and then to plan the LRV sorties and the scientific activity. Easily identifiable craters and other prominent features are located, the sorties are planned using these as check-points, relief models are made, and the crew is trained into familiarity with the area.

The relevance of this to the LRV is simply that adequate navigation by landmarks and by use of the pictorial high accuracy maps of the area should be entirely possible. Navigation accuracy by the MCC-H and/or the crew using the visual check points could be quite good. Additionally the LM should be easily visible at distances of at least 1 KM and probably as much as 3KM. (Recall that the crew should not go further away than 9.5 KM.) The top of the LM descent stage is 3.1 meters high and the top of the LM ascent stage is 6.0 meters. The distance R to the lunar horizon from an object of height h is of the form $R = 1864 \sqrt{h}$, with h and R in meters. Thus, if the surface is smooth, a man 2 meters high can see the top of the descent stage from 5.9 KM away, and the top of the ascent stage from 7.2 KM away, quite comfortable distances.

But the surface is probably not smooth. Figure 4 shows what height obstacle, placed as unfavorably as possible, could obstruct vision. Four heights are given for the LM - as if it rests below, on or above the average surface. Similarly, three heights for the observer are given: we remark

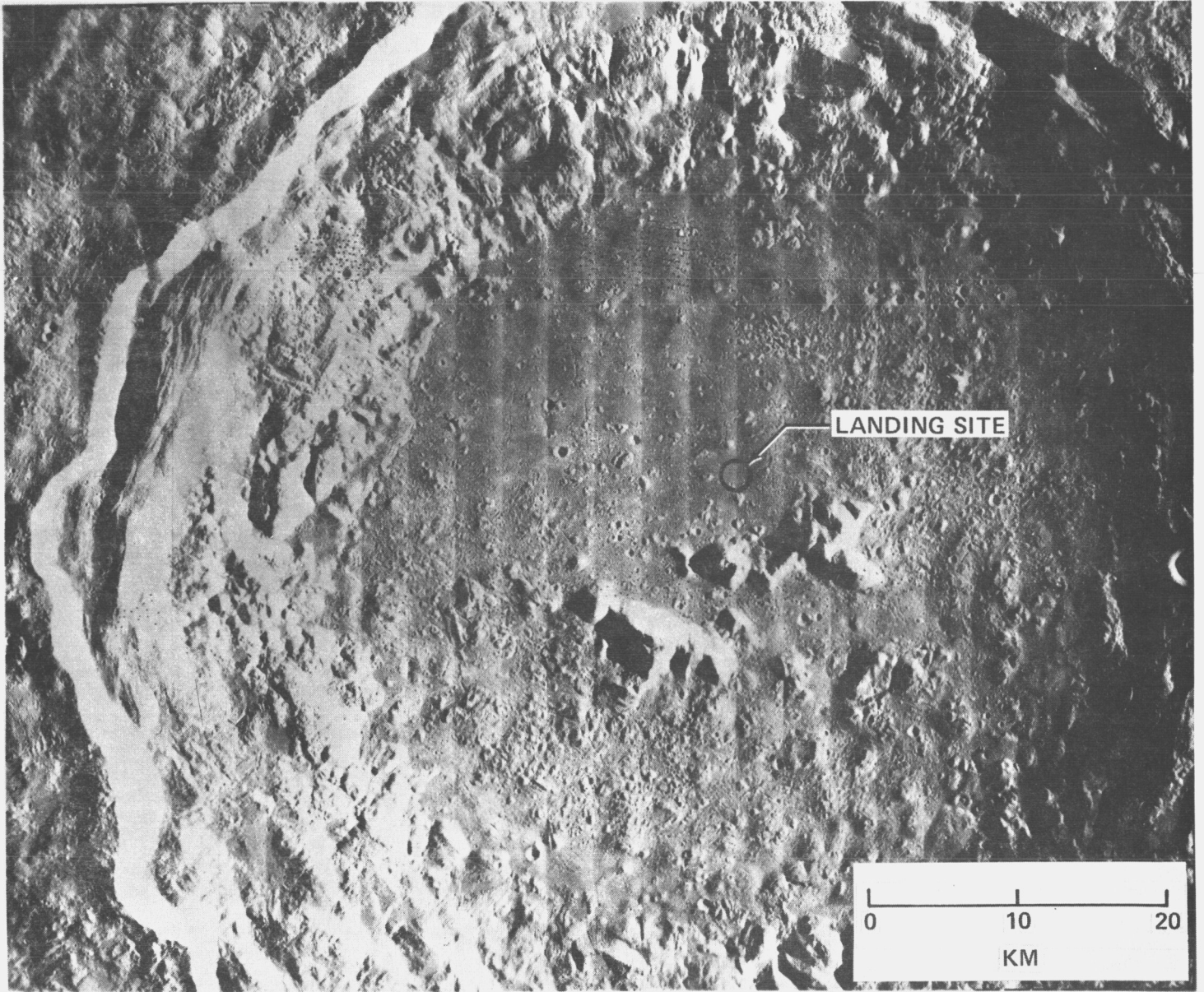


FIGURE 2 - COPERNICUS PEAKS

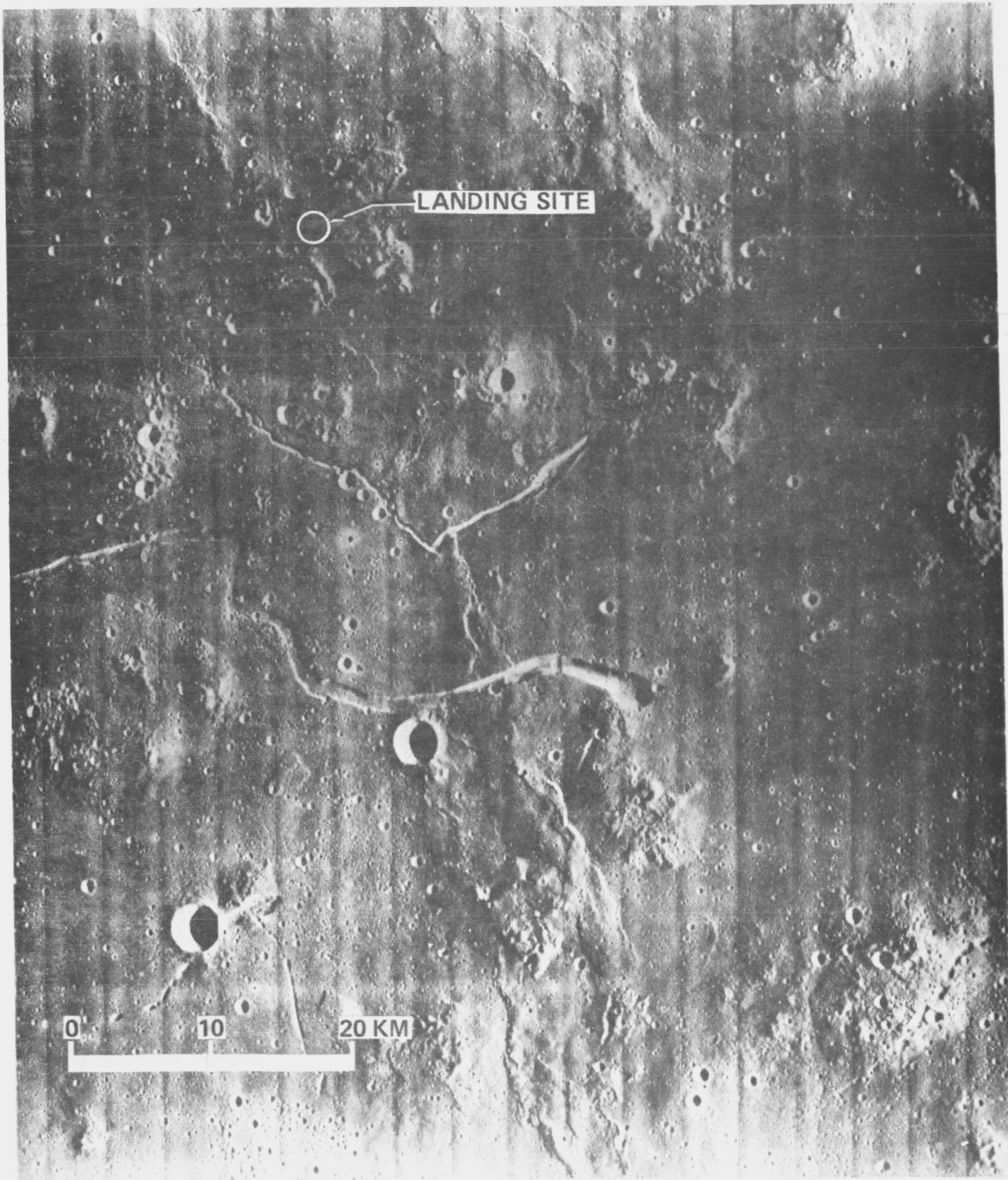


FIGURE 3 - MARIUS HILLS

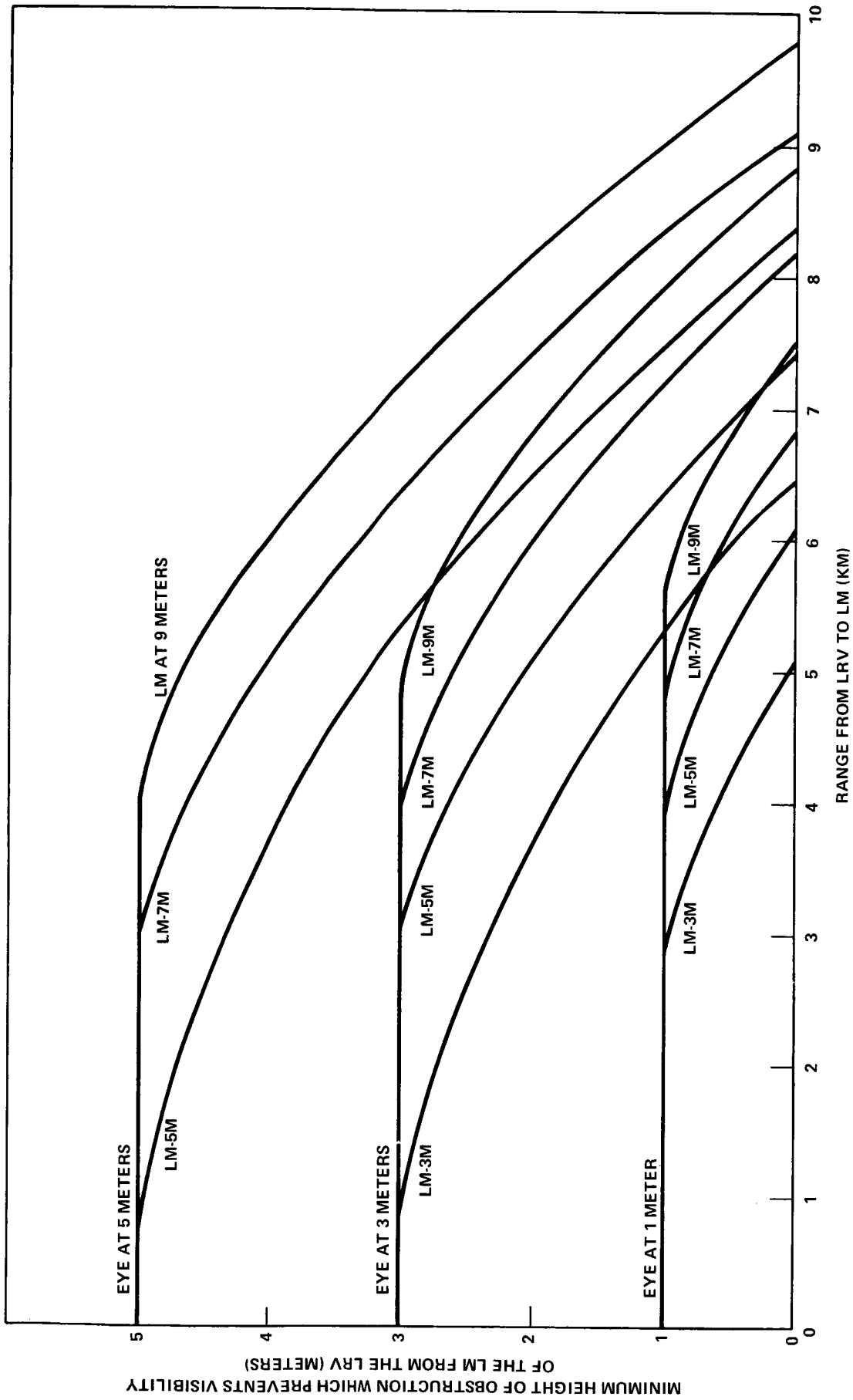


FIGURE 4 - HEIGHT OF OBSTRUCTION WHICH PREVENTS VISIBILITY OF LM FROM THE LRV VS. RANGE

it is a natural policy to stand on the LRV or climb whatever hill is convenient when trying to see a goodly distance. Thus, the figure shows, for the LM at 3 meters, the LRV range at 4000 meters, and the eye at 1 meter, that an obstacle about 0.6 meters high (not 1 because of the curvature of the moon) will obscure visibility of the LM, but if the eye is raised to 3 meters, the required obstacle size increases to about 1.8 meters. An obstacle of such height may be either a rock (in which case the proper procedure is to drive on with the LRV to another vantage point), or a ridge (which if it runs for an appreciable distance is a useful landmark for navigation without need to see the LM). Navigation using the visual check-points until the LM is visible should be completely acceptable.

So it appears that the LRV navigation system is not a mandatory system and that mission rules should permit sorties whether it is operable or not. Its convenience must be weighed against the time diverted from primary sortie tasks to keep it operating. The accuracy requirements placed on it must balance between being accurate enough to be useful, but not so stringent that it requires continual crew attention (in realigning the directional gyro). On such balance, 700 meters (1σ) seems to be a reasonable requirement.* Ten deg/hr gyro drift, 3° gyro alignment accuracy, and 3 realignments made conveniently during a sortie are needed to achieve this accuracy (see following sections). With such accuracy, and reasonable LM visibility, no travel should be wasted in returning to the LM.

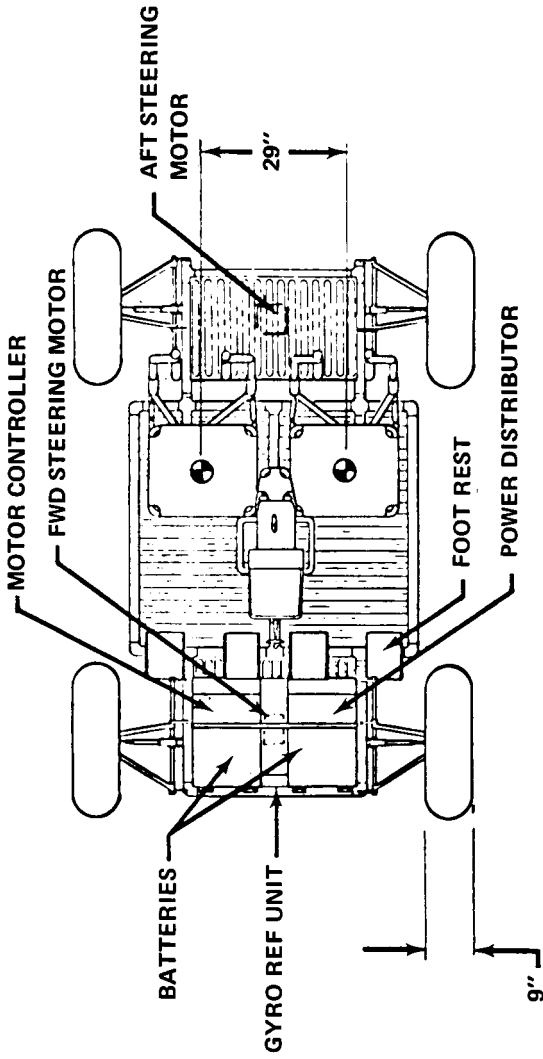
Specification accuracy requirements are equivalent to 850 meters, and the system can be expected to perform appropriately (or better) to its function.

3.0 FUNCTIONAL DESCRIPTION OF THE NAVIGATION SYSTEM

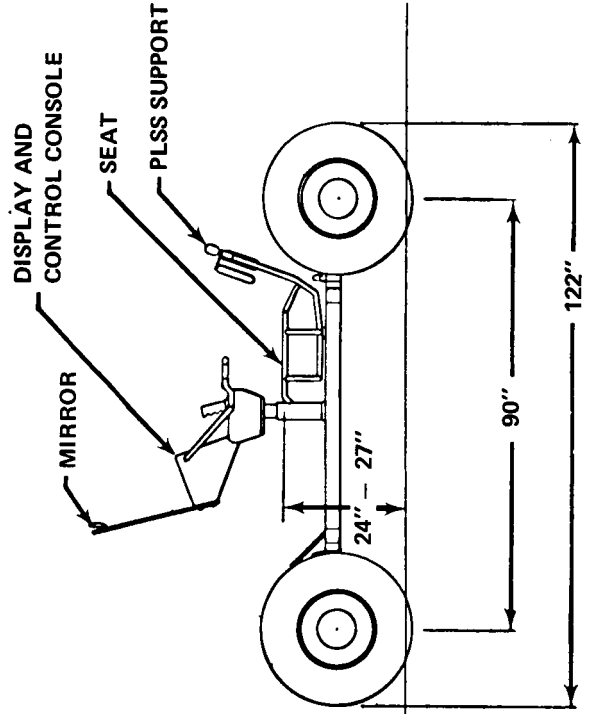
Figure 5 shows three views of the Lunar Roving Vehicle. The control console which contains the navigation display and the control panel is located on a pedestal between the two astronauts. As shown in Figure 6, the panel contains readouts of range to the LM (XX.X KM), bearing to the LM (XXX. deg), traverse distance (XX.X KM), directional gyro gimbal angle (Heading, in 1° markings), and a velocity meter. The power, system reset and gyro torquing switches are all pull-before-throw type controls.

To align or realign the directional gyro, the LRV is driven so that the sun is within $\pm 15^\circ$ of dead aft, shining over the shoulders of the astronauts. The gnomon of the

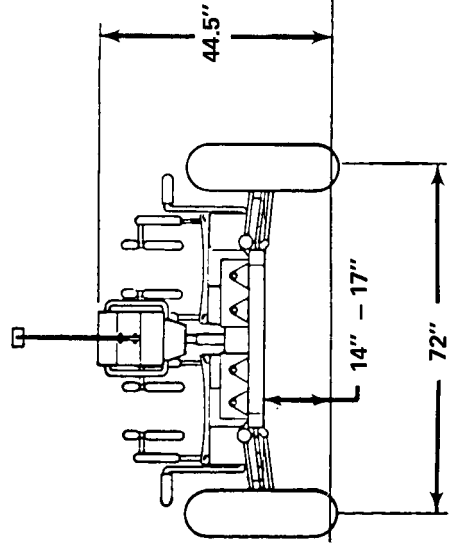
*The LRV can drive 700 meters in about 5 minutes. Walking, some 10-15 minutes would be required, if such a navigation error could go unnoticed until the end.



PLAN VIEW



SIDE VIEW



FRONT VIEW

FIGURE 5 - LUNAR ROVING VEHICLE

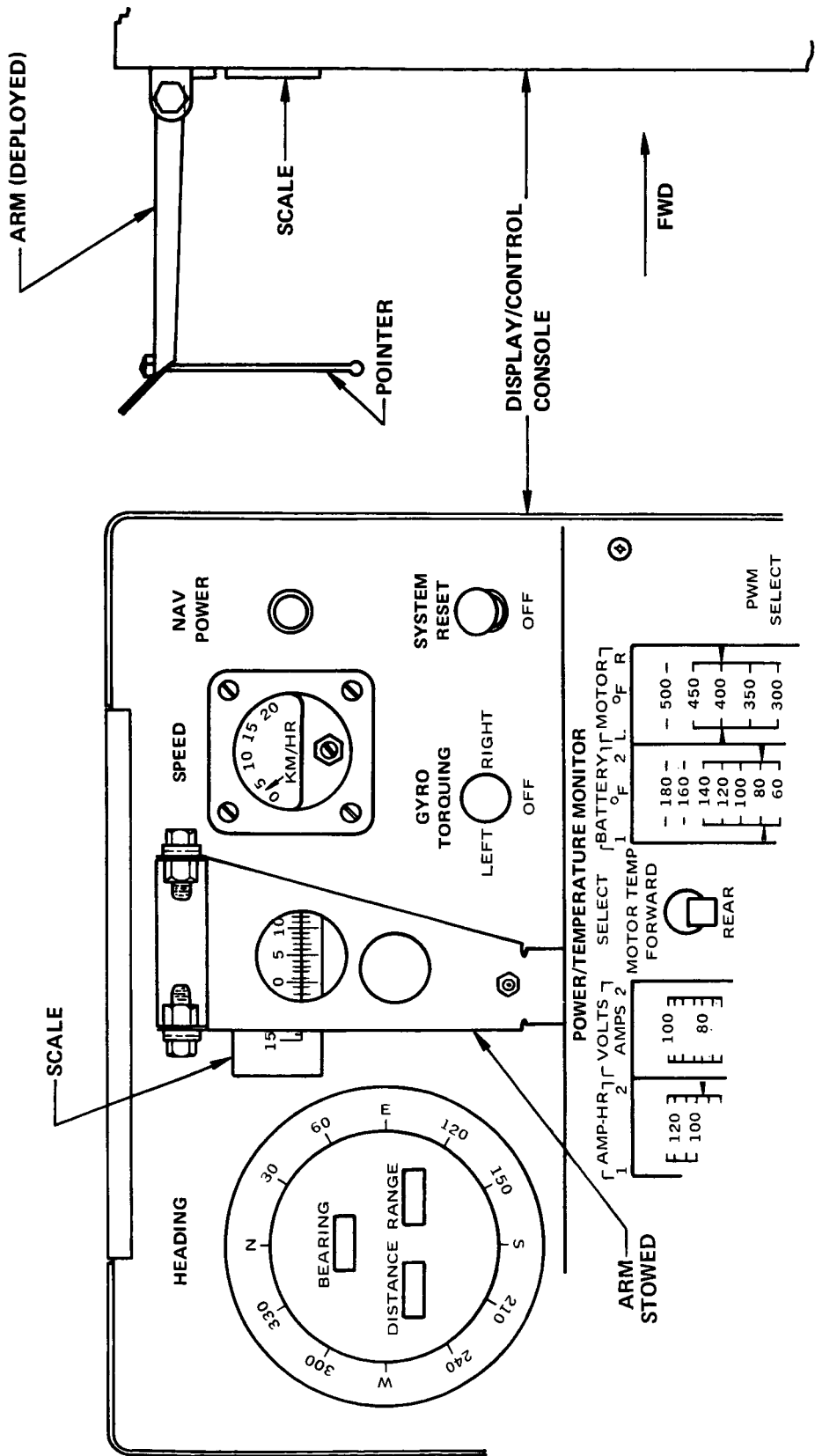


FIGURE 6 - SUN SHADOW DEVICE

sundial is then rotated into position so that its shadow falls on the $\pm 15^\circ$ Sun Shadow Device (S.S.D.) scale affixed to the console. The gnomon is stored in a folded position inside the console for protection against being bent or causing damage to the crew pressure suits. The crew reads and passes to the Mission Control Center-Houston (MCC-H) the S.S.D. angle, and the LRV pitch and roll angles. The pitch and roll angles are obtained from a simple pendulum device on the left side of the console (as shown in Figure 7).

The MCC-H uses these angles and sun and moon ephemeris data to calculate the directional gyro gimbal (Heading) angle so that the gyro is correctly aligned with lunar North. This angle is voiced to the LRV crew and set on the Heading indicator via the gyro torquing control.

Range, Bearing and Distance Counters are initialized with the system reset control and the sortie can begin. To measure distance, each wheel has nine equally spaced magnetic devices mounted on it. As the wheels rotate, these devices pass stationary reed switches and trigger pulses which are sent to the computer. A composite pulse occurs at the time when the third wheel puts out its third pulse. The composite pulse is scaled to 0.735 meters in the computer. Requiring pulses from three wheels eliminates the effects of wheel slip in two wheels. Not requiring a pulse from the fourth wheel is an attempt to avoid the effects of a single device failure.

The 0.735 meter distance (pulse) granularity includes natural wheel deformation and nominal slip correction factors. Each 0.735 meter distance increment is resolved into North-South and East-West components using the sine and cosine of the heading angle. These are extracted by a Scott "T" network from the directional gyro selsyn output. Accumulator digital registers hold the North-South, East-West position of the LRV with respect to the LM. The cartesian position data is then converted to polar form (Range and Bearing to LM) by a novel technique called the Cordic Algorithm.[1] This uses addition and digital shifting processes to convert cartesian coordinates to polar coordinates without using the Pythagorean theorem or arc-tangent functions. As a result it saves considerable computer complexity.

Range and Bearing to the LM are displayed for the crew on the digital counters shown in Figure 6. These counters are reset only when the system reset switch is used. If LRV power or navigation system failure occurs, the counters are not automatically reset. The only capability of the reset switch is to zero the counters, hence no position corrections can be made during a traverse even if landmark and/or MCC-H position data are available.

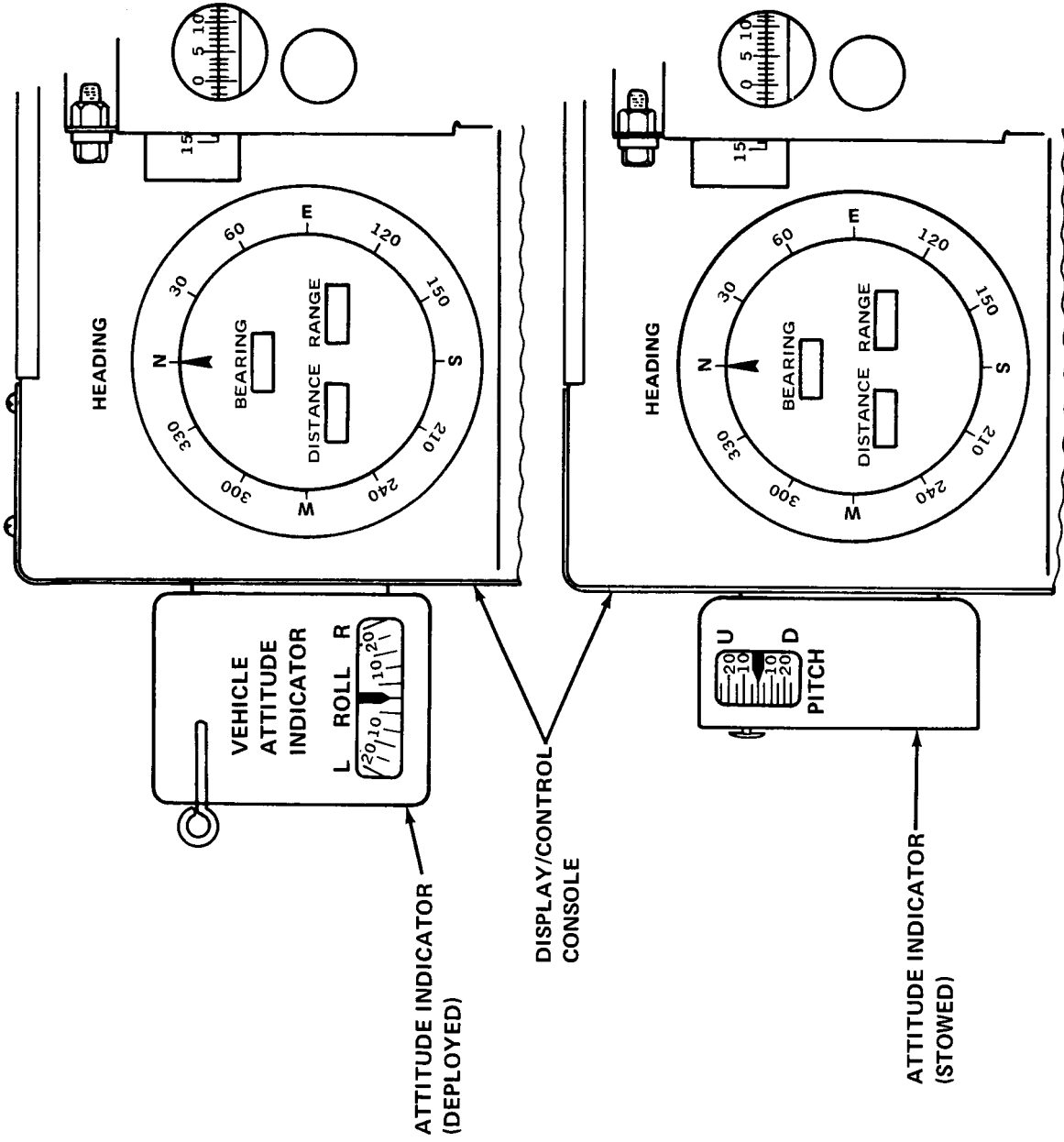


FIGURE 7 - VEHICLE ATTITUDE INDICATOR

Periodically the gyro is realigned to correct for its drift since the last alignment. How often alignment needs to be done is a function of the gyro drift rate and the LM relative location accuracy required. Realignment should not be needed so often that it interferes with the purposes of the sortie.

The DIST (distance traveled) readout is used mainly as an indicator of how much traverse capability (battery power) has been used, and thus is an indication of the remaining travel capability of the LRV.

More detailed data on the Signal Processing Unit and the Directional Gyro Unit can be obtained from Reference 2.

4.0 WHEEL PULSE ACCURACY EFFECTS

The nine magnetic devices on each wheel should pose no problem in accurate mounting: slight inaccuracies will have a negligible overall effect. The wheels are fairly compressible, and load variations (rock samples, for instance) will change the effective wheel radius. Also producing errors will be the effect of soft soil which induces churning and, most certainly, wheel slip. These effects will be amplified as the LRV negotiates slopes. The technique of requiring odometer pulses from three wheels to generate one composite pulse will help the odometer error situation somewhat, but anything which similarly affects more than two wheels induces an error into the navigation system.

The North/South position (N) and the East/West position (E) can be written as:

$$N = \int_0^t V \cos H \, dt$$

$$E = \int_0^t V \sin H \, dt$$

Where V is the LRV velocity and H is its direction (azimuth, East of lunar North).

Actually this is a discrete equation because the distance is measured in pulses. But the pulses come so close together that there is no significant difference between the results of the two forms.

Defining a scale factor F as a number normally equal to 1.0, varying as the wheel size varies, and defining a slip velocity S as motion of the wheels without motion of the LRV (with S desirably zero), the true equations are

$$N_T = \int_0^t (FV+S) \cos H \, dt$$

$$E_T = \int_0^t (FV+S) \sin H \, dt.$$

or, expanded,

$$N_T = \int_0^t FV \cos H \, dt + \int_0^t S \cos H \, dt$$

$$E_T = \int_0^t FV \sin H \, dt + \int_0^t S \sin H \, dt.$$

The LRV path returns to its starting point, i.e., ideally $\int_0^t V \cos H \, dt$ and $\int_0^t V \sin H \, dt$ equal zero at the end of the sortie. Thus if F is a constant, an error in wheel size will have no effect at the end of the sortie, there is simply a rescaling of distance. At other times, the error will be the difference in F from unity times the North or East position (if F is constant). If F is variable, the error could be greater or less than such a value depending on the variation in F and when it happens.

A constant slip S is equivalent to a variation in F , but it is most likely a variable. It depends on slope and terrain softness.

Analysis by The Boeing Co. based on a variation in wheel size of 1% gives an error of some 50 meters for the reference sortie. Analysis continues to determine the proper values to use, but they are difficult to quantify precisely because they depend also on the soil and terrain along the actual path of the LRV. But the next section shows gyro alignment errors to be much greater than 50 meters: unless present estimates of wheel size variations and slip are grossly in error, these factors will not contribute important errors.

5.0 GYRO ALIGNMENT ACCURACY EFFECTS

Assuming that the azimuth angle H is in error by a small amount ΔH , the N and E equations become, approximately:

$$N = \int_0^t V \cos H \, dt - \int_0^t (\Delta H) V \sin H \, dt$$

$$E = \int_0^t V \sin H \, dt + \int_0^t (\Delta H) V \cos H \, dt.$$

or, for the errors

$$\epsilon_N = - \int_0^t (\Delta H) V \sin H \, dt$$

$$\epsilon_E = + \int_0^t (\Delta H) V \cos H \, dt.$$

Since the LRV returns to its starting point, constant values of ΔH will cause no error at the end of the sortie, the effect being only a small rotation of coordinate axes.

But this is not the likely case. One expects the alignment error at each realignment to be random, and uncorrelated with the error at any other realignment. Additionally, the gyro will

probably drift, the value being approximately constant throughout the sortie. Under such assumptions we write, for the period between the i th and $(i+1)$ st realignment, the equations (ΔH_o = alignment error, D = drift rate)

$$\Delta H = \Delta H_{o,i} + D(t-t_i)$$

$$\epsilon_{N,i} = - \Delta H_{o,i} \int_{t_i}^{t_{i+1}} V \sin H dt - D \int_{t_i}^{t_{i+1}} (t-t_i) V \sin H dt$$

or

$$\epsilon_{N,i} = + \Delta H_{o,i} [E(t_i) - E(t_{i+1})] + D[-(t_{i+1} - t_i) E(t_{i+1}) + \int_{t_i}^{t_{i+1}} E(t) dt]$$

$$\epsilon_{E,i} = + \Delta H_{o,i} [N(t_{i+1}) - N(t_i)] + D[(t_{i+1} - t_i) N(t_{i+1}) - \int_{t_i}^{t_{i+1}} E(t) dt]$$

For compactness, write these equations as

$$\epsilon_{N,i} = \Delta H_{o,i} a_i + D b_i$$

$$\epsilon_{E,i} = \Delta H_{o,i} c_i + D d_i$$

The cumulative error at the k th alignment time (or at time t_k) is then

$$\epsilon_{N,k} = \sum_{i=1}^k (\Delta H_{o,i} a_i + D b_i)$$

$$\epsilon_{E,k} = \sum_{i=1}^k (\Delta H_{o,i} c_i + D d_i)$$

To develop statistical measures, the assumptions are (with $\bar{\quad}$ indicating expected value):

$$\bar{D} = D, \quad \overline{D^2} = D^2, \quad \overline{\Delta H_{O,i}} = 0, \quad \overline{\Delta H_{O,i}^2} = \sigma^2$$

$$\overline{D \Delta H_{O,i}} = 0 \quad \overline{\Delta H_{O,i} \Delta H_{O,j}} = 0 \text{ for } i \neq j$$

With the results, for the mean value

$$\overline{\epsilon_{N,k}} = D \sum_{i=1}^k b_i$$

$$\overline{\epsilon_{E,k}} = D \sum_{i=1}^k d_i$$

and for the standard deviation

$$\overline{(\epsilon_{N,k} - \overline{\epsilon_{N,k}})^2} = \sigma^2 \sum_{i=1}^k (a_i)^2$$

$$\overline{(\epsilon_{E,k} - \overline{\epsilon_{E,k}})^2} = \sigma^2 \sum_{i=1}^k (c_i)^2$$

Figure 8a plots these effects for drift rates of 10 deg/hr and alignment errors of 3 degrees for the reference sortie shown there. East and North errors have been root-sum-squared to remove any effect due to the specific orientation of the sortie. The data are given for 0 to 5 realignments equally spaced during the sortie (a time of 2.5 hours was used, which represents the time actually spent moving - a science stop for a significant time without realigning the gyro will put these data in error), and the errors are shown for four times during the sortie.

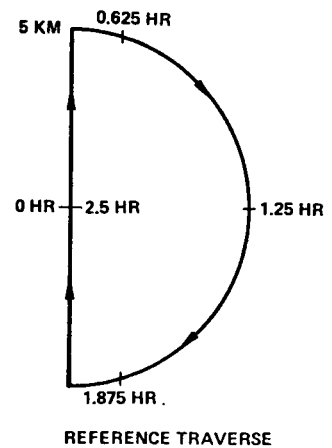
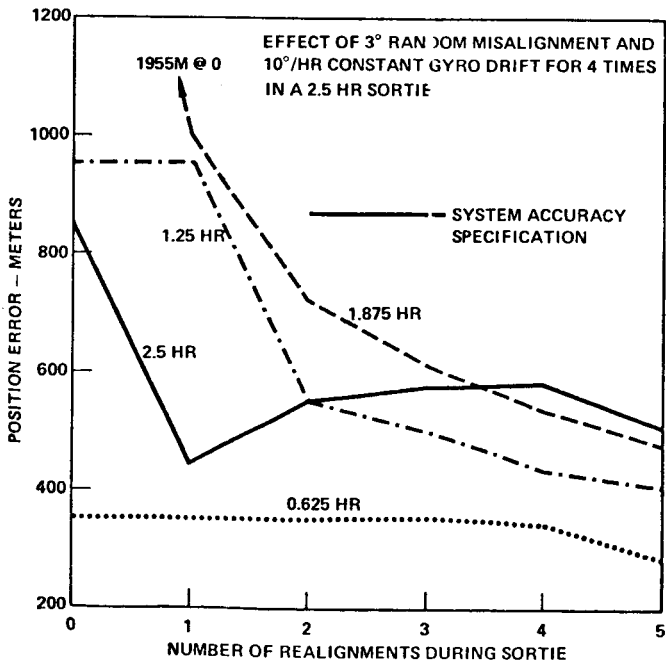
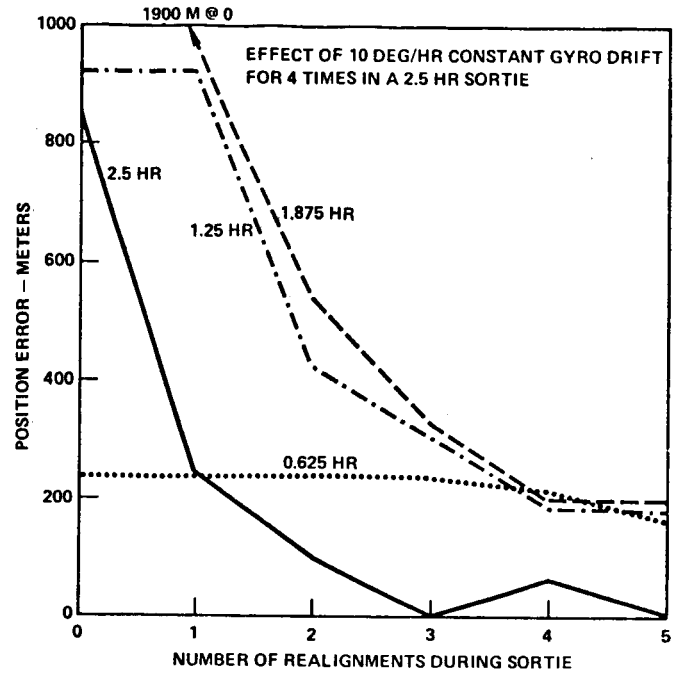
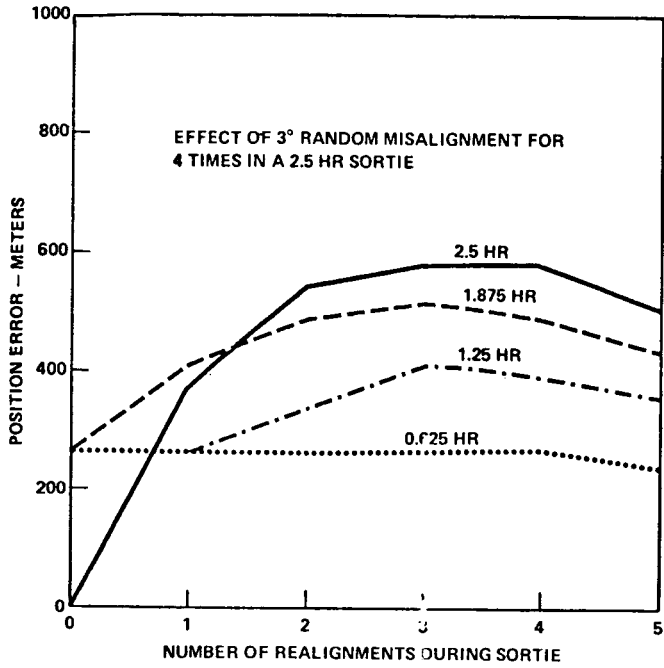


FIGURE 8A - GYRO ERROR EFFECTS FOR A REFERENCE MISSION

The errors scale directly with misalignment and drift rate values. Three degree misalignment and $10^\circ/\text{hr}$ give approximately equal errors and are achievable, which is why these specific values were used.

The results are somewhat surprising: one would expect the error to reduce the more frequent the realignments. But the special shape of the sortie path - that it returns to its starting point - upsets this intuitive estimate unless there are more realignments than it is practical to make. This is why the errors are given at four different times - to avoid being misled by the effects of the path shape.

Since the drift rate, although constant during any sortie, will likely be random from one sortie to the next, it is reasonable to root-sum-square the errors due to misalignment and drift, and this result is also plotted. Three realignments are better than 2 and about the same as 4 and therefore an accuracy goal of 700 meters, with 3° alignment error and $10 \text{ deg}/\text{hour}$ drift rate seems reasonable and achievable without difficulty.

Figure 8b gives the same type of data for a straight line sortie of 10 KM of 2 hours duration. The errors are similar and the same conclusions can be reached.

6.0 GYRO ALIGNMENT DETERMINATION TECHNIQUES

To reduce the effect of gyro drift, the directional gyro can be realigned when the LRV stops for scientific purposes. To begin a realignment, the LRV is driven until the sun is within $\pm 15^\circ$ of dead aft. The gnomon of the Sun Shadow Device (see Figure 6) is then rotated until its shadow falls on the scale. The scale angle (called D° in this section), the pitch angle P of the LRV, the roll angle R , and the directional gyro angle G' are then voiced to the MCC-H. MCC-H uses sun ephemeris data (azimuth ψ and elevation θ at the present time at the LM's location)* to calculate a new angle G , to which the directional gyro is torqued. Comparing G' before realignment with G gives an idea of gyro drift rate (see later).

Analysis shows accuracy in LRV pitch and roll to be reasonably important (also see later). Therefore, the readings and gyro torquing should take place with the crew in place, and preferably just before the LRV resumes the sortie. Taking readings before science activity begins and torquing the gyro after science activity ends is not recommended, because the pitch and roll angles might change.

*LM or LRV - the difference in their locations is insignificant here.

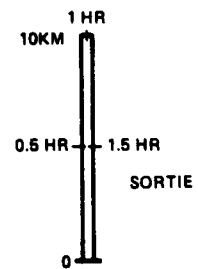
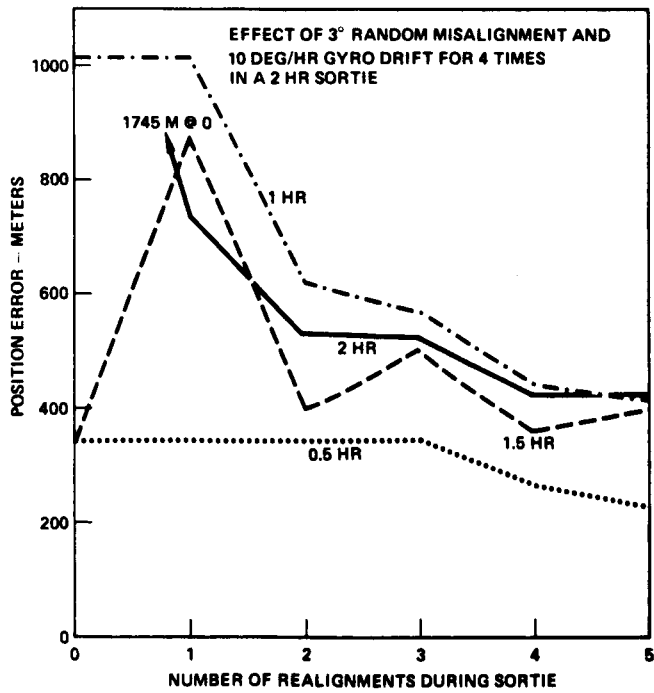
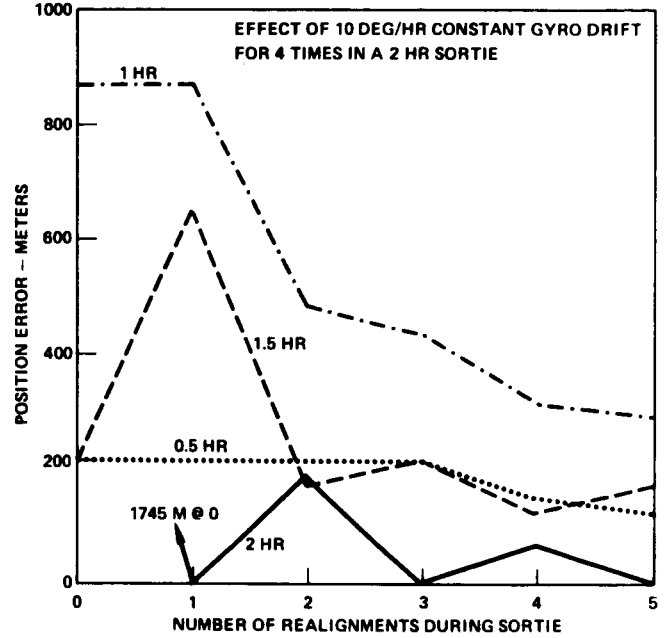
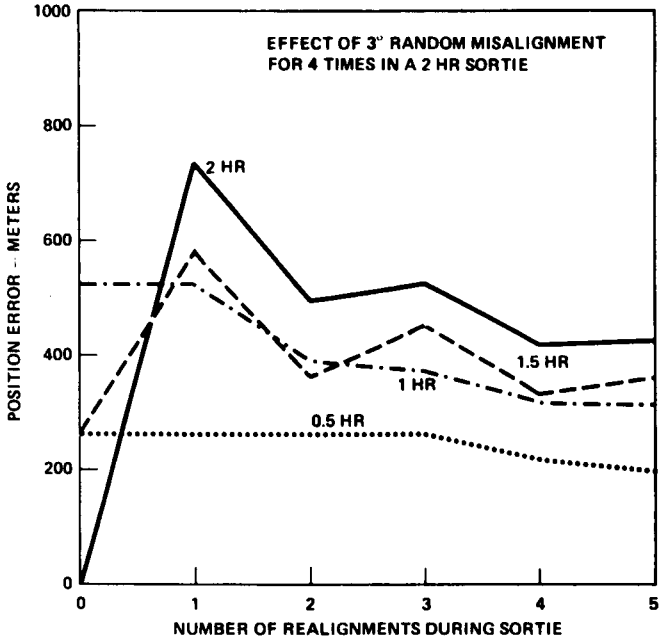


FIGURE 8B - GYRO ERROR EFFECTS FOR A STRAIGHT LINE SORTIE

Analysis also shows that the scale reading D° is not generally an accurate measure of the azimuth angle between the sun and the LRV. The correct formula is developed in the following sections, an accurate approximate formula and nomographs are then developed, and remarks are made on the effects of errors.

6.1 The Sun Shadow Device

Figure 9 shows the elements of the Sun Shadow Device and gives dimensions. It indicates why the accuracy of the S.S.D. is a function of sun elevation. The pivot of the bracket is not at the scale and consequently the distance between the gnomon and the scale varies with sun elevation and LRV pitch. The scale is calibrated for a sun elevation angle of about 25° , but is 33% in error at a sun elevation angle of 60° . Further, roll of the LRV offsets the reading by about a factor of unity at a sun elevation angle of 45° .

The true relationship between D° , the scale reading, and the variables ψ (sun azimuth relative to lunar North), θ (sun elevation angle above horizontal), H (LRV heading from lunar North), A (relative heading of the LRV to the sun, see Figure 10), P (LRV pitch angle), R (LRV roll angle) and B (gnomon bracket angle, see Figure 9) is found by solving the vector equation shown in Figure 9 for c (where the sun ray which casts a shadow on the scale hits the gnomon), d (distance from the gnomon to the scale), and r (the scale reading in inches) which is related to D° by the formula

$$D^\circ = r/0.05767.$$

The formulas* are shown in Figure 11.

*The Eulerian angle P used here is theoretically different from the angle P read from the instrument, but the difference is far less than the precision with which the angle can be read.

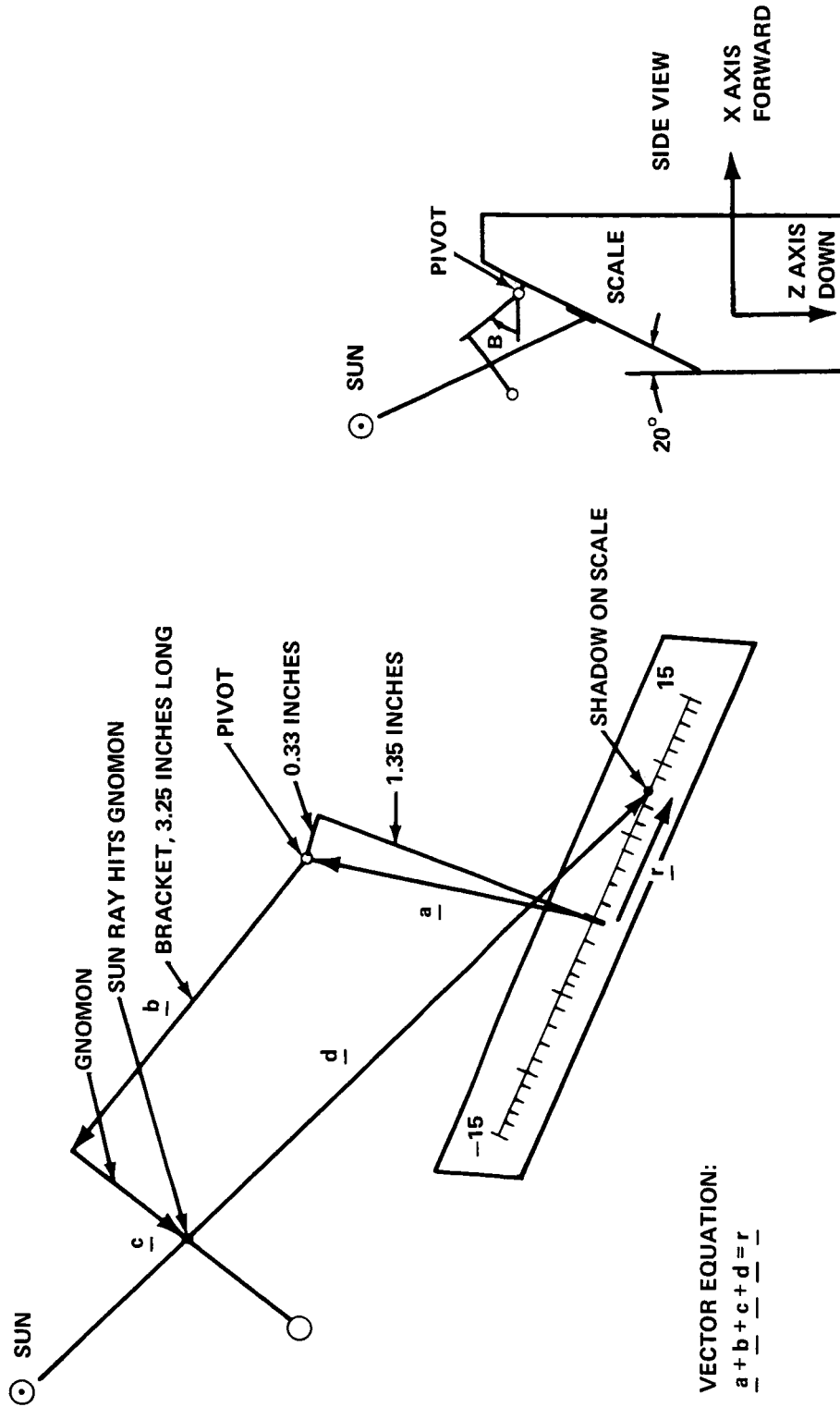
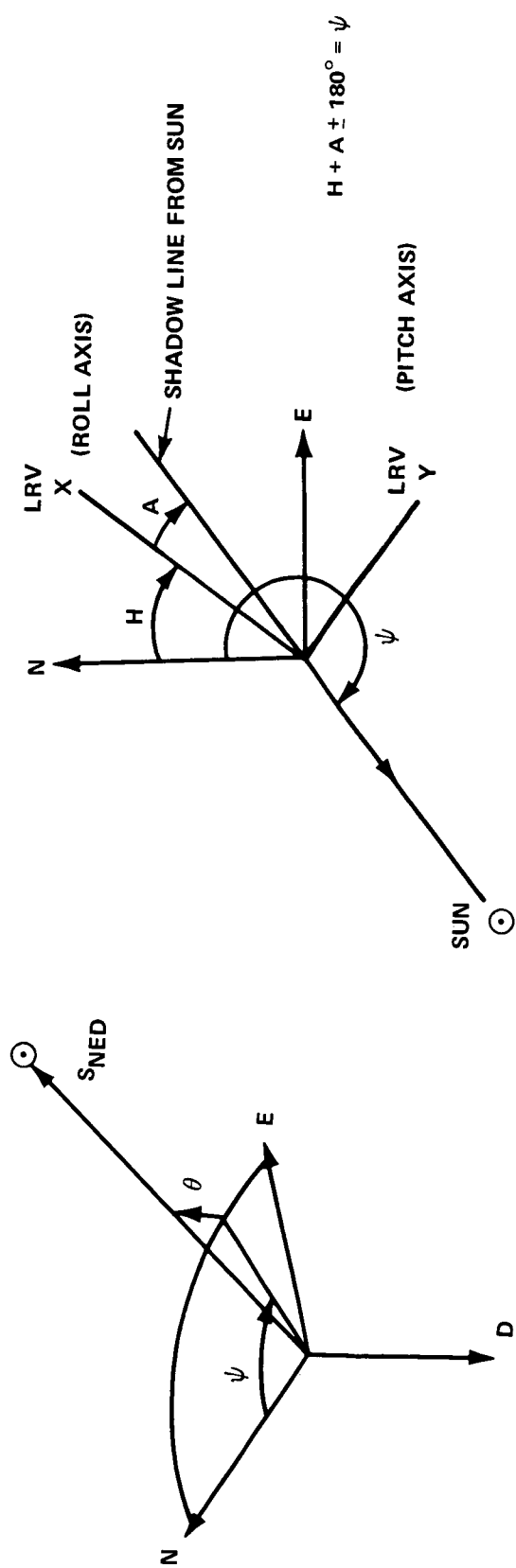


FIGURE 9 - SUN SHADOW DEVICE GEOMETRY FOR EXACT SOLUTION



LOCATING THE SUN

DEFINITION OF ANGLES

FIGURE 10 - DEFINITION OF ANGLES

Calculate:

$$\alpha = 1.35 \sin 20^\circ - 0.33 \cos 20^\circ$$

$$\beta = -1.35 \cos 20^\circ - 0.33 \sin 20^\circ$$

$$S_X = -C_A C_\theta C_P - S_\theta S_P$$

$$S_Y = C_A C_\theta S_P S_R + S_A C_\theta C_R + S_\theta C_P S_R$$

$$S_Z = C_A C_\theta S_P C_R - S_A C_\theta S_R + S_\theta C_P C_R$$

Iterate the following two equations, varying B until c = 1.1 (middle of gnomon)

$$\text{Det} = S_X \cos B + S_Z \sin B$$

$$c = (\alpha S_Z - \beta S_X) / \text{Det}$$

Then complete the calculations with

$$d = (\alpha \cos B + \beta \sin B - 3.25) / \text{Det}$$

$$D^\circ = -S_Y d / 0.05767$$

Figure 11 - Algorithm to compute the S.S.D. Scale Reading D°

The computational procedure is to vary the angle B (by a Newton-Raphson iteration procedure, for example) until $C = 1.1''$, which is the mid-point of the gnomon.

A true sundial would give $D^\circ = A^\circ$, but for the reasons noted above, the S.S.D. is not a true sundial. Figure 12 shows the error $D - A$ vs. A for a variety of sun elevation angles, and with LRV pitch and roll both zero. The error approaches 5° at high sun angles. Figure 13 shows $D - A$ vs. A again but now for a pitch angle of $+5^\circ$ and a roll angle of -5° . Now the maximum error is 11° . Corrections for sun elevation and LRV pitch and roll are obviously necessary.

A policy of limiting relative sun azimuth to $\pm 5^\circ$ instead of $\pm 15^\circ$ has been discussed. This reduces the 11° error to 8° , not enough benefit to make the policy desirable. A later section shows the full $\pm 15^\circ$ can be used with little error.

6.2 Sun Azimuth and Elevation

A few words about sun azimuth and elevation may be appropriate here, to establish the ranges of interest. Reference 4 has been used.

Relative to the moon's equator and pole, the sun's period in longitude is 29.5 days (0.508 degrees/hour). In latitude, the sun varies over a range of $\pm 1.6^\circ$, with a period of about 346 days.

For an Apollo mission, the sun elevation angle is restricted to being greater than about 7° at landing, and to less than about 60° at the end of a 66 hour stay time with a T + 24 hour launch. The maximum elevation angle also depends on the latitude of the site, which varies between about $+25^\circ$ (Hadley-Apennines, Apollo 15) and about -10° (Davy)--these being the northern- and southern-most sites under present consideration.

Figure 14 shows variations of sun azimuth ψ and elevation θ with time for some of the missions of present interest. It also shows the change in sun azimuth during 5 hours (representing the maximum duration of a sortie). The sun stays between -20° and $+40^\circ$ of East, and may change as much as 3° in azimuth during a sortie, a change large enough not to be neglected. It is not difficult, however, to precalculate these angles for specific missions, and simply tabulate them.

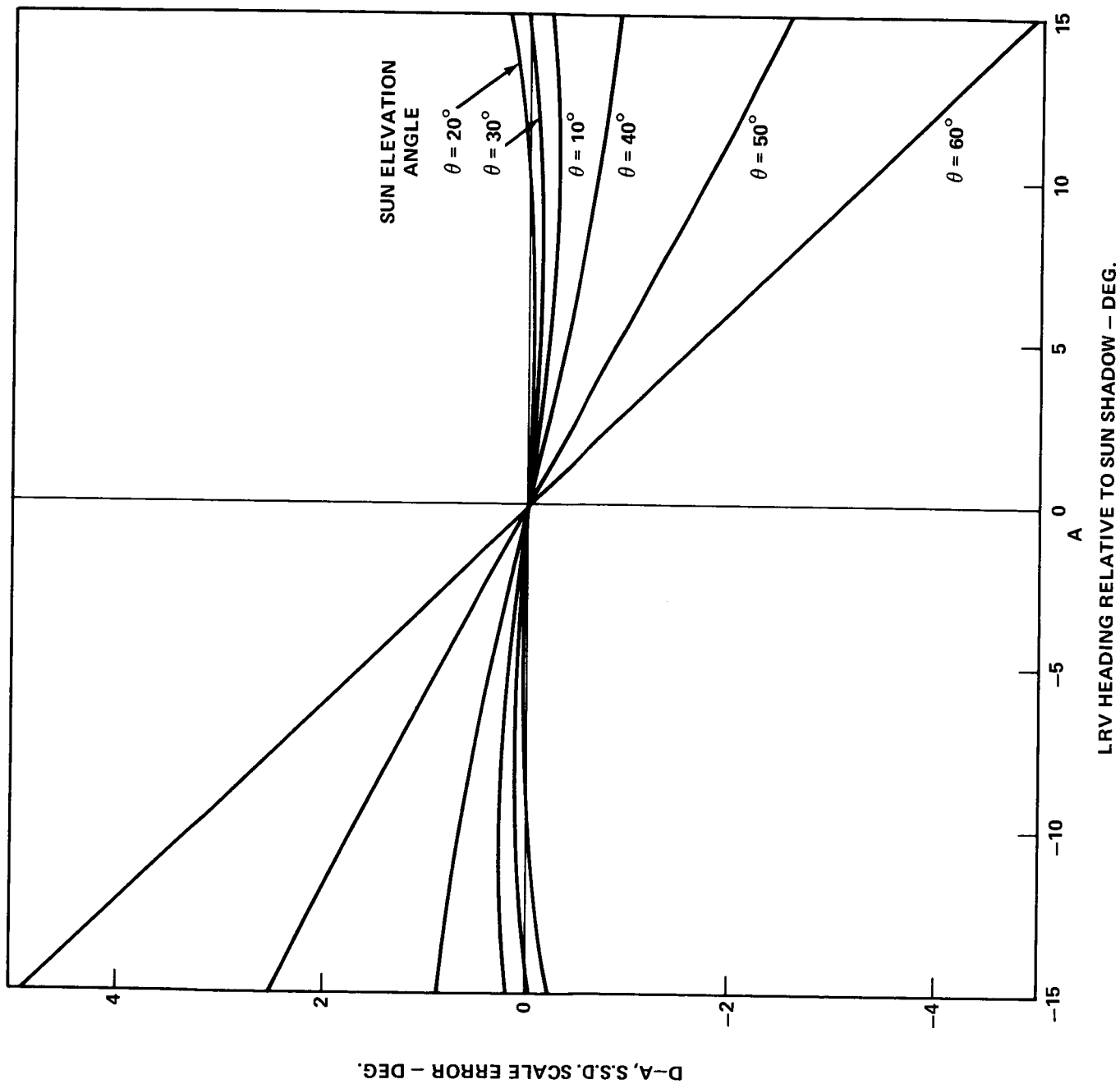
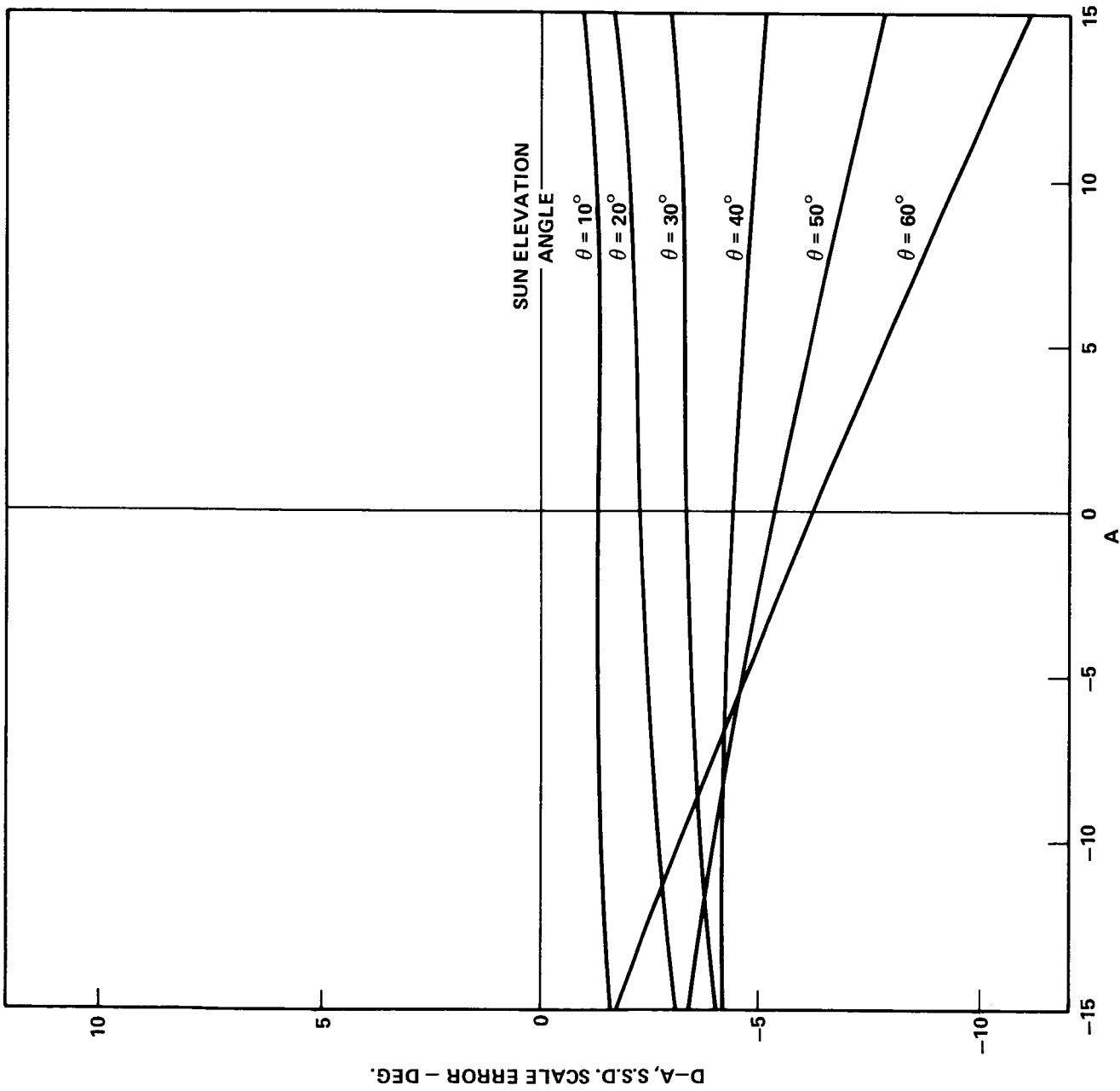
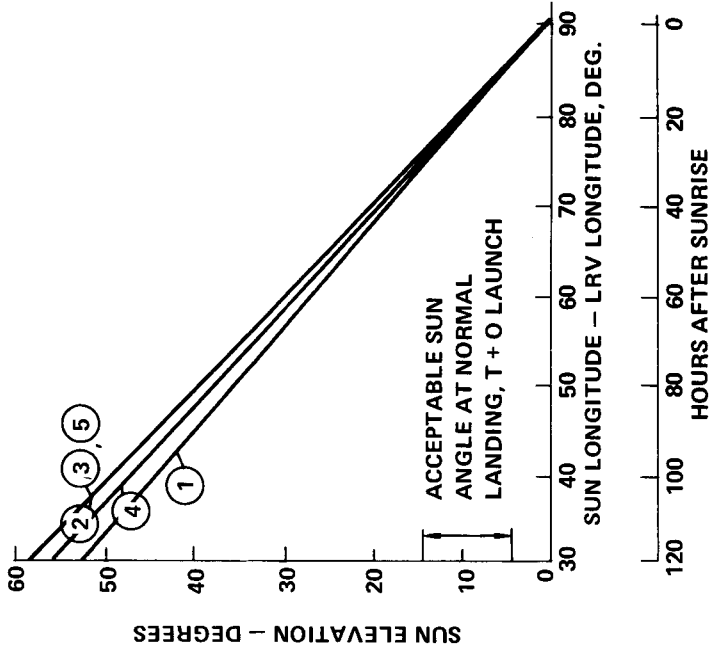


FIGURE 12 - S.S.D. SCALE ERROR, PITCH AND ROLL BOTH ZERO



LRV HEADING RELATIVE TO SUN SHADOW - DEG.

FIGURE 13 - S.S.D. SCALE ERROR, PITCH 5° , ROLL -5°



KEY

- 1 HADLEY - JULY, 1971
 - 2 DESCARTES - JAN., 1972
 - 3 COPERNICUS - JAN., 1972
 - 4 MARIUS HILLS - JUNE, 1972
 - 5 DAVY - JUNE, 1972
- MAXIMUM SURFACE STAY TIME - 66 HOURS

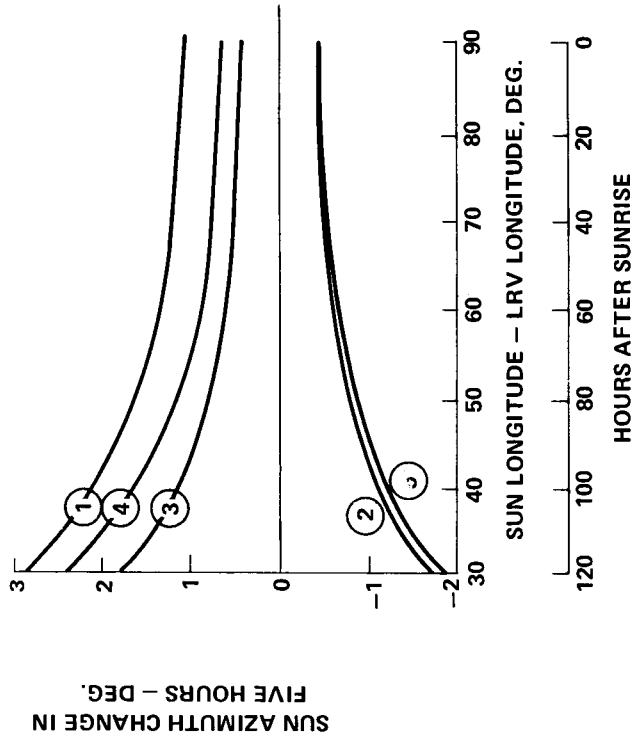
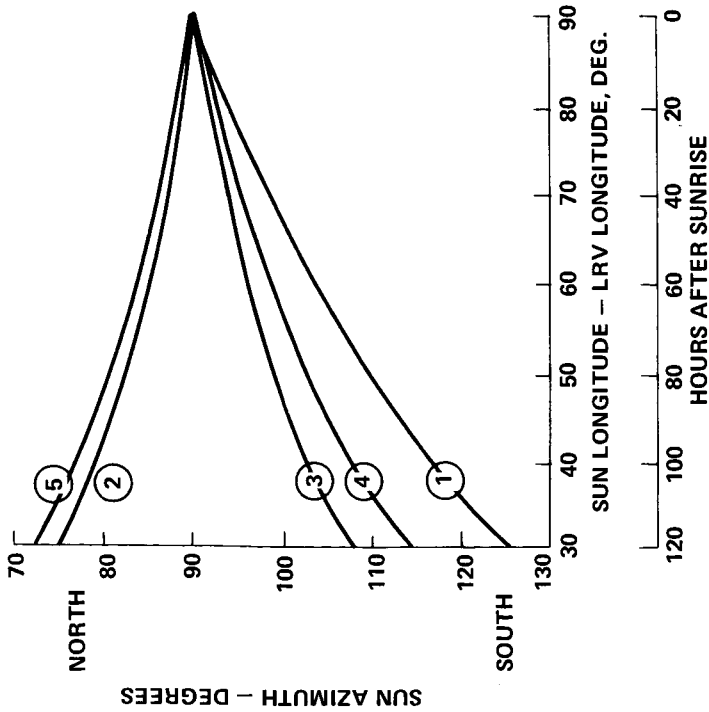


FIGURE 14 - SUN AZIMUTH AND ELEVATION VARIATIONS

6.3 Sun Shadow Device Nomographs

Two methods are possible for processing the data given by the crew: using the RTCC computers, or nomographs and tables. Figure 15 gives a routine for the RTCC which has been tested by the writers with perfect results, given perfect data. It is a Newton-Raphson iteration based on the formulas given earlier.

Nomographs can be developed easily if small angle assumptions ($\cos = 1$, $\sin = \text{angle}$) are made for the angles A, R and Δ . Δ appears in the approximation

$$B = \theta + P + \Delta, \Delta < 10^\circ$$

The analysis first uses the equation for c given earlier to find Δ , and then substitutes this in the equation for D, solving it for A. The resulting formulas are (with α and β as before)

$$f(\theta+P) = \frac{(180/\pi) (0.05767)}{(3.25 - \alpha C_{\theta+P} - \beta S_{\theta+P}) + (\alpha S_{\theta+P} - \beta C_{\theta+P}) (1.1 - \alpha S_{\theta+P} + \beta C_{\theta+P}) / 3.25}$$

$$A_1^\circ = \frac{D^\circ f(\theta + P)}{C_\theta}$$

$$A_2^\circ = -R^\circ S_{\theta+P} / C_\theta$$

$$A^\circ = A_1^\circ + A_2^\circ$$

(θ , ψ from tables,
D, P, R read by
crew S = sin,
C = cosine)

$$H = \psi - A \pm 180^\circ$$

The function $f(\theta+P)$ is plotted in Figure 16. Nomographs, based on techniques given in Reference 5 are given in Figures 17 and 18. They are surprisingly accurate: given

$$\begin{aligned}\alpha &= 1.35 \sin 20^\circ - 0.33 \cos 20^\circ \\ \beta &= -1.35 \cos 20^\circ - 0.33 \sin 20^\circ \\ r &= D^\circ(0.05767) \text{ (converts sundial angle to inches on the scale)} \\ B &= \theta + P \text{ (first guess)} \\ A_C &= D^\circ \text{ (first guess)}\end{aligned}$$

$$\textcircled{1} S_X = -C_{A_C} C_\theta C_P + S_\theta S_P$$

$$S_Y = -C_{A_C} C_\theta S_P S_R - S_{A_C} C_\theta C_R - S_\theta C_P S_R$$

$$S_Z = -C_{A_C} C_\theta S_P C_R + S_{A_C} C_\theta S_R - S_\theta C_P C_R$$

$$\text{Det} = S_X \cos B + S_Z \sin B$$

$$\epsilon_c = c_d - (S_Z(\alpha - 3.25 \cos B) - S_X(\beta - 3.25 \sin B))/\text{Det}$$

$$\epsilon_r = r + S_Y(\alpha \cos B + \beta \sin B - 3.25)/\text{Det}$$

$$\frac{dS_X}{dA} = +S_{A_C} C_\theta C_P$$

$$\frac{dS_Y}{dA} = +S_{A_C} C_\theta S_P S_R - C_{A_C} C_\theta C_R$$

$$\frac{dS_Z}{dA} = +S_{A_C} C_\theta S_P C_R + C_{A_C} C_\theta S_R$$

$$\begin{aligned}\frac{d\epsilon_c}{dA} &= -[(\alpha - 3.25 \cos B) \frac{dS_Z}{dA} - (\beta - 3.25 \sin B) \frac{dS_X}{dA}] / \text{Det} \\ &\quad + (c_d - \epsilon_c) \left(\frac{dS_X}{dA} \cos B + \frac{dS_Z}{dA} \sin B \right) / \text{Det}\end{aligned}$$

$$\frac{d\epsilon_c}{dB} = -3.25(S_Z \sin B + S_X \cos B)/\text{Det} + (c_d - \epsilon_c)(-S_X \sin B + S_Z \cos B)/\text{Det}$$

$$\frac{d\epsilon_r}{dA} = \frac{dS_Y}{dA} (\alpha \cos B + \beta \sin B - 3.25)/\text{Det} + (r - \epsilon_r) \left(\frac{dS_X}{dA} \cos B + \frac{dS_Z}{dA} \sin B \right) / \text{Det}$$

$$\frac{d\epsilon_r}{dB} = S_Y (-\alpha \sin B + \beta \cos B)/\text{Det} + (r - \epsilon_r) (-S_X \sin B + S_Z \cos B)/\text{Det}$$

$$\begin{bmatrix} P_{11} & P_{12} \\ P_{21} & P_{22} \end{bmatrix} = \begin{bmatrix} d\epsilon_c/dA & d\epsilon_c/dB \\ d\epsilon_r/dA & d\epsilon_r/dB \end{bmatrix}^{-1} \quad \text{(Invert the matrix)}$$

$$\begin{bmatrix} \Delta A \\ \Delta B \end{bmatrix} = - \begin{bmatrix} P_{11} & P_{12} \\ P_{21} & P_{22} \end{bmatrix} \begin{bmatrix} \epsilon_c \\ \epsilon_r \end{bmatrix}$$

$$A_C = A_C + \Delta A$$

$$B = B + \Delta B$$

If $(|\Delta A| < \text{tolerance A})$ and $(|\Delta B| < \text{tolerance B})$ exit, otherwise return to $\textcircled{1}$.

Figure 15 - Algorithm for complete compensation for pitch, roll, and S. S. D. Geometry

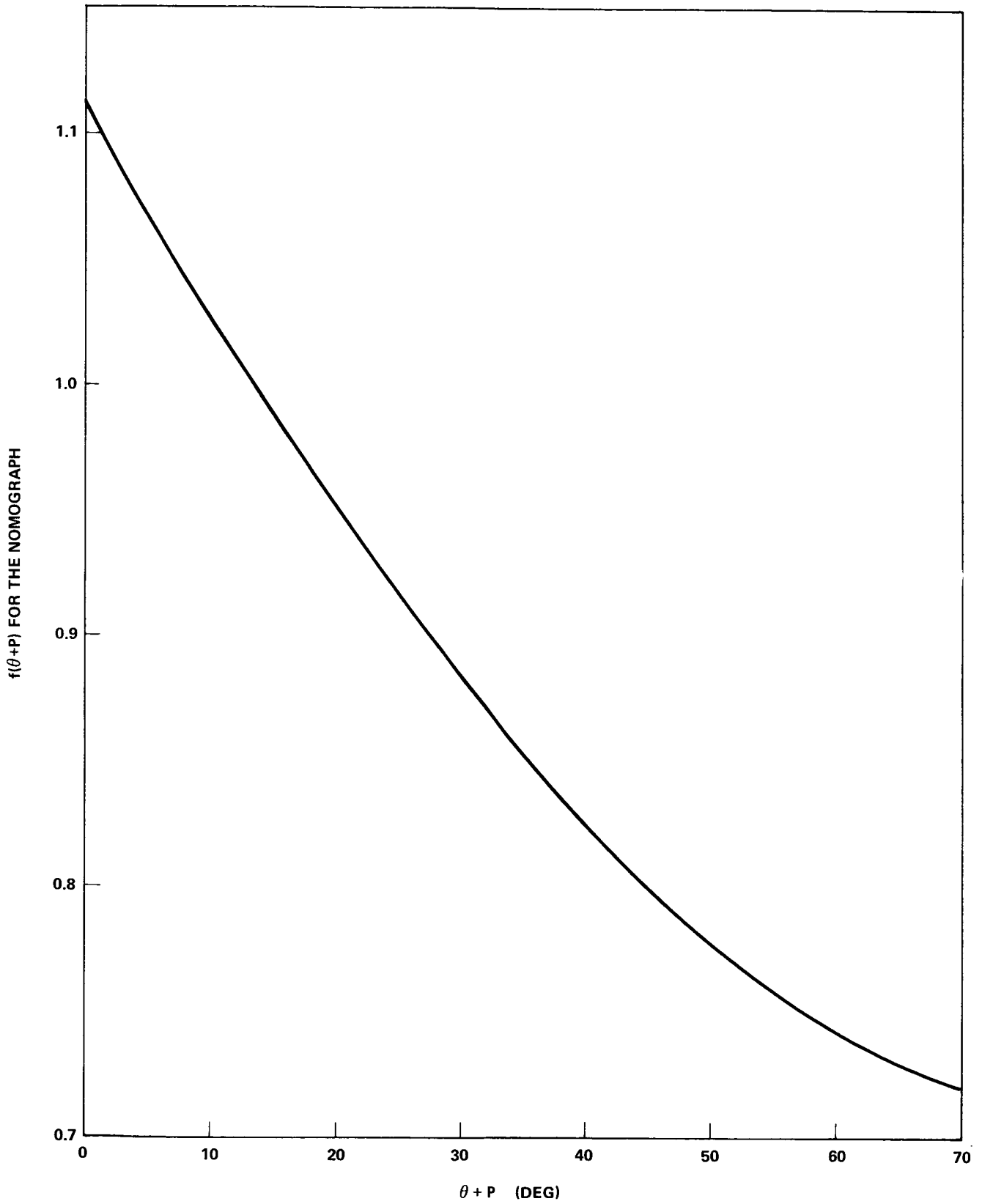


FIGURE 16 - THE FUNCTION $f(\theta+P)$ FOR THE NOMOGRAPH

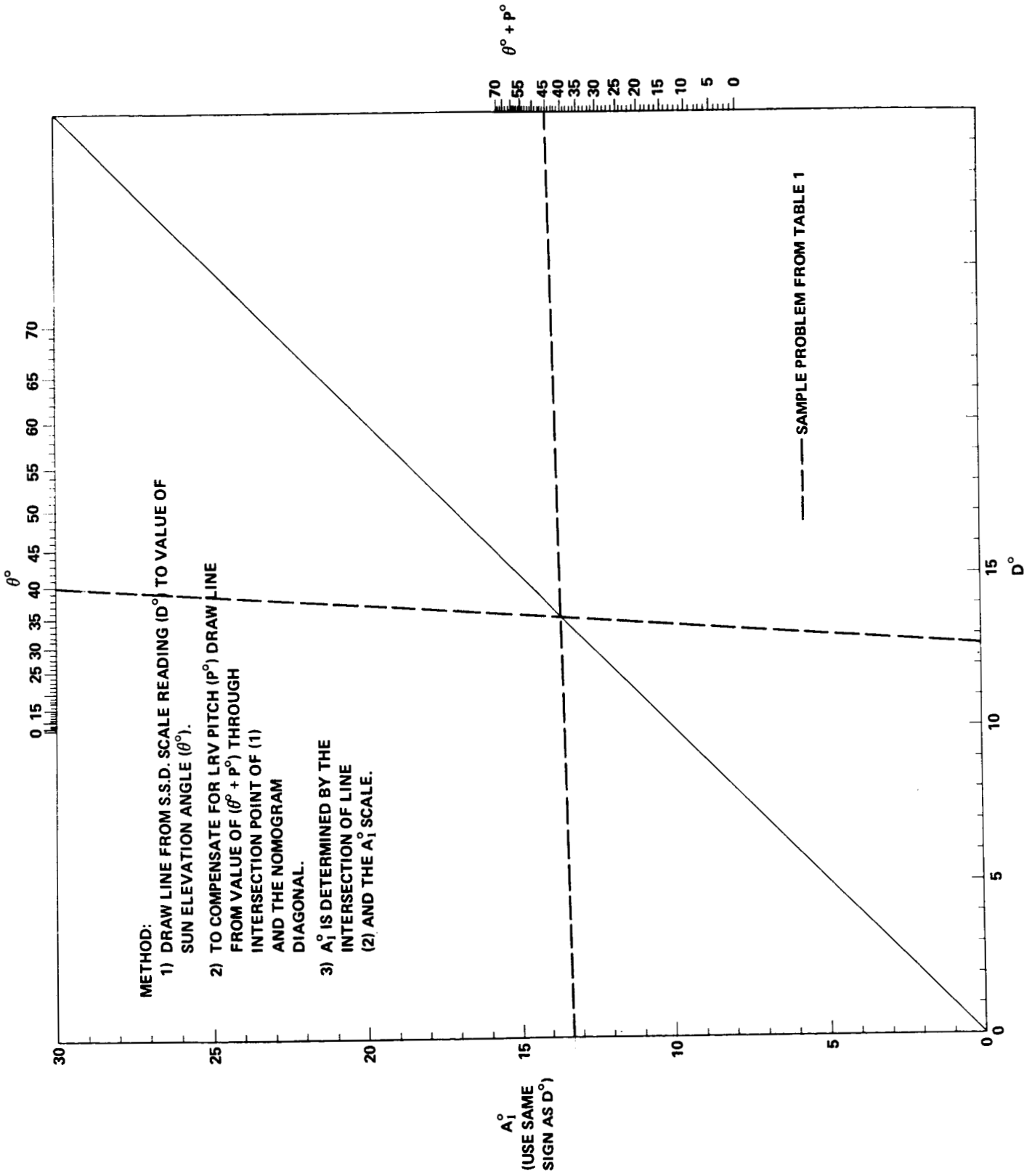


FIGURE 17 - NOMOGRAM FOR A_1°

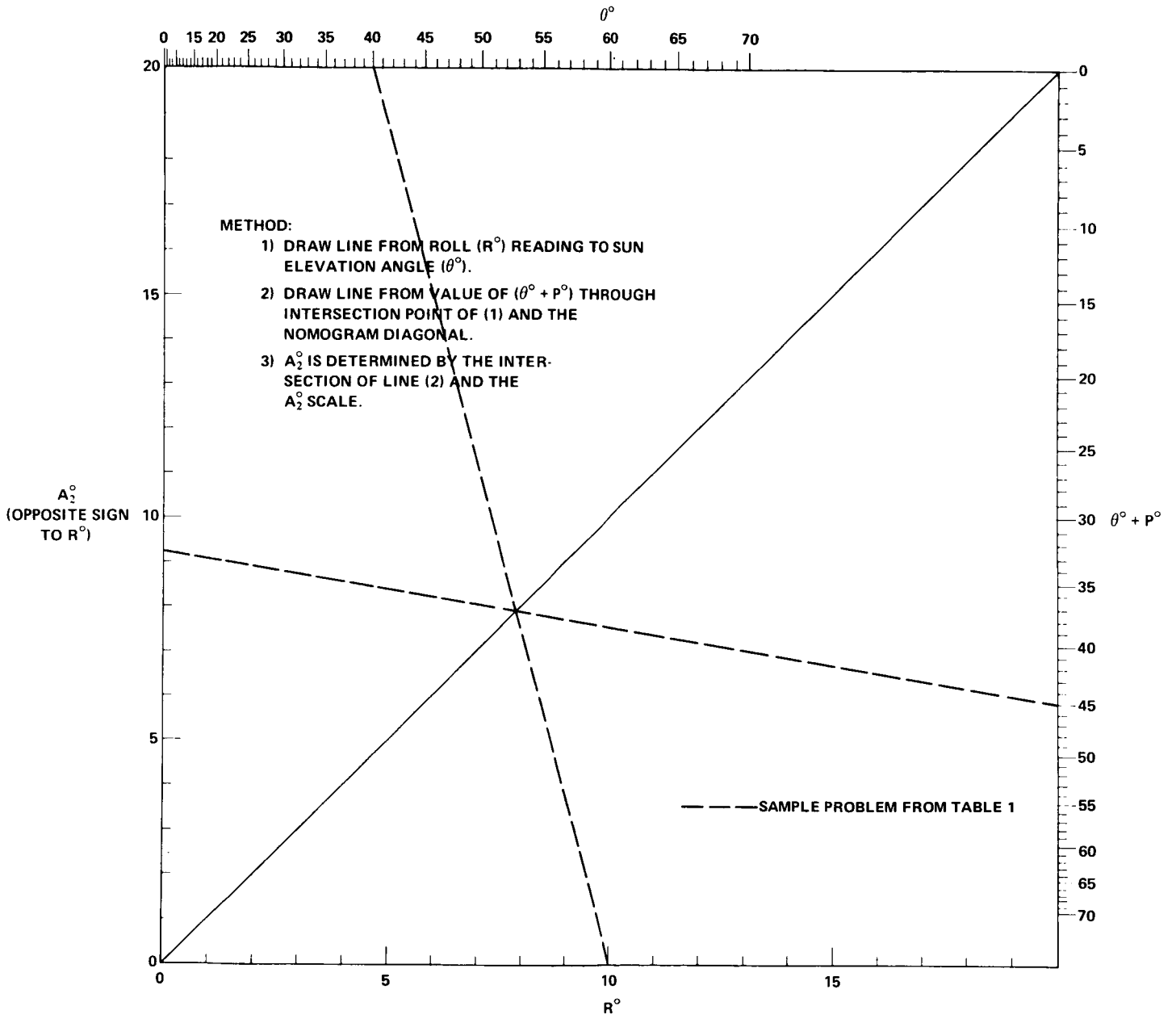


FIGURE 18 - NOMOGRAM FOR A_2°

perfect data, the error is less than 0.5° for all cases in the ranges $P \pm 10^\circ$, $R \pm 10^\circ$, $D \pm 15^\circ$ and θ 10° to 60° . It is generally less than 0.2° , reaching 0.5° only for $\theta=60^\circ$ and $P=\pm 10^\circ$, $R=\pm 10^\circ$.

Table 1 gives sample data and a worksheet so the reader can try the procedures noted in the nomographs.

The small angle assumption could also be made for the pitch angle but the error rises to as much as 2° . The ease of using the nomographs makes this additional approximation unnecessary, and actually simplifies the work.

6.4 Directional Gyro Angle Nomograph

The angle H is not exactly equal to the directional gyro angle G if the LRV angles P and R are not zero. The formula is

$$G = \arctan \frac{S_H C_R - C_H S_P S_R}{C_H C_P}$$

If $P=R=0$, the formula shows that $G=H$, as expected.

If the small angle ϕ is defined by

$$G = H + \phi$$

then ϕ is given accurately by

$$\phi^\circ = -P^\circ R^\circ C_H^2 / (180/\pi)$$

Figure 19 is a nomograph for this equation. It is used after H is calculated.

To check gyro drift, assume the reading of the direction gyro angle before realignment is G' . Inverting the G equation, find H' from

$$H' = \arctan \frac{S_{G'} C_P + C_{G'} S_P S_R}{C_{G'} C_R}$$

Table 1

θ°	P°	R°	D°	A_{true}°	A_1°	A_2°	A°	ψ°	H°	ϕ°	G°
10	-10	5	-13.75	-15.00	-15.49	0	-15.49	100	- 64.51	.16	- 64.35
20	10	-10	-13.10	- 7.00	-12.31	5.32	- 6.99	40	-133.01	.81	-132.20
20	- 5	- 5	9.27	11.00	9.74	1.38	11.12	130	- 61.12	-.10	- 61.22
30	5	10	- 3.30	-10.00	- 3.25	-6.67	- 9.92	80	- 90.08	.00	- 90.08
30	-10	5	2.71	1.00	2.97	-1.97	1.00	120	- 61.00	.21	- 60.79
40	5	10	12.69	4.00	13.27	-9.23	4.04	135	- 49.04	-.38	- 49.42*
40	-10	10	- 2.87	-10.00	- 3.31	-6.53	- 9.84	110	- 60.16	.43	- 59.73
40	5	- 5	7.99	13.00	8.36	4.62	12.97	90	-102.97	.02	-102.95
50	- 5	- 5	-10.90	- 8.00	-13.58	5.50	- 8.08	115	- 56.92	-.13	- 57.05
50	10	- 5	3.63	11.00	4.20	6.74	10.94	115	- 75.94	.05	- 75.89
60	5	5	.08	- 9.00	.12	-9.06	- 8.95	35	-136.05	-.23	-136.28
60	- 5	5	- 4.36	-15.00	- 6.63	-8.19	-14.82	105	- 60.18	.11	- 60.07

*Case plotted in figures 17, 18, 19.

Work Form

$\theta =$	$A_1 =$	$\psi =$
(add) $P =$	(add) $A_2 =$	(sub) $A =$
$(\theta+P) =$	$A =$	<u>±180.00</u>
$D =$		$H =$
$R =$		(add) $\phi =$
		$G =$

and compare H' with H to measure gyro drift. Note, however, that moon rotation over a period of time is equivalent to gyro drift (the amount is $0.0508 \sin(\text{latitude})$ deg/hour) and such effects must be removed before drift can be calculated.

6.5 Effects of Errors

The nomographs also make it relatively easy to calculate the effects of errors in reading D , P and R . Figure 20 shows that A_1 (and A) is changed by 1.7° by a 1° error in D . Figure 21 shows that A_1 is changed by 0.6° by a 5° error in P (an exaggerated pitch error to make the figure easier to read). And Figure 22 shows A_2 changed by 2° by a 1° error in R . Although these are extreme cases, the sensitivity to roll errors and the accuracy of the nomograms, etc. suggests 3° as a reasonable accuracy to expect.

Assumed in all the above formulas is that the center of the gnomon is used ($c = 1.1$ in the formulas). It is important that this be done--the scale reading can change by up to 2° if either end is actually used instead of the center (if the MCC-H assumes the center has been used). A reasonable tolerance is about ± 0.2 " of the center; and the crew should be cautioned to observe it.

Care should also be taken not to bend or twist the bracket or gnomon. The scale uses 0.05767 " per degree--if the gnomon moves by this much, a rather small amount, the reading will change by 1° and, in general, H will change by more than 1° . The bracket appears fairly rugged, but the small diameter required for the gnomon makes it fairly fragile, especially considering the heavy gloves worn by the crew. The crew must be cautioned to treat it carefully. Perhaps tabs should be added to the bracket to make it easier to handle without touching the gnomon, and the strength of the gnomon base increased by flanges.

Moving the scale closer to the pivot of the bracket was considered as a possible means of improving the S.S.D. But reflecting on the strong effects of LRV roll (as in the A_2 nomograph), such measures would not help much. Function $f(\theta+P)$ cannot be made equal to a simple constant of unity without drastic redesign, using the nomographs cannot be avoided, and so there is no particular value in attempting to improve the configuration of the S.S.D.

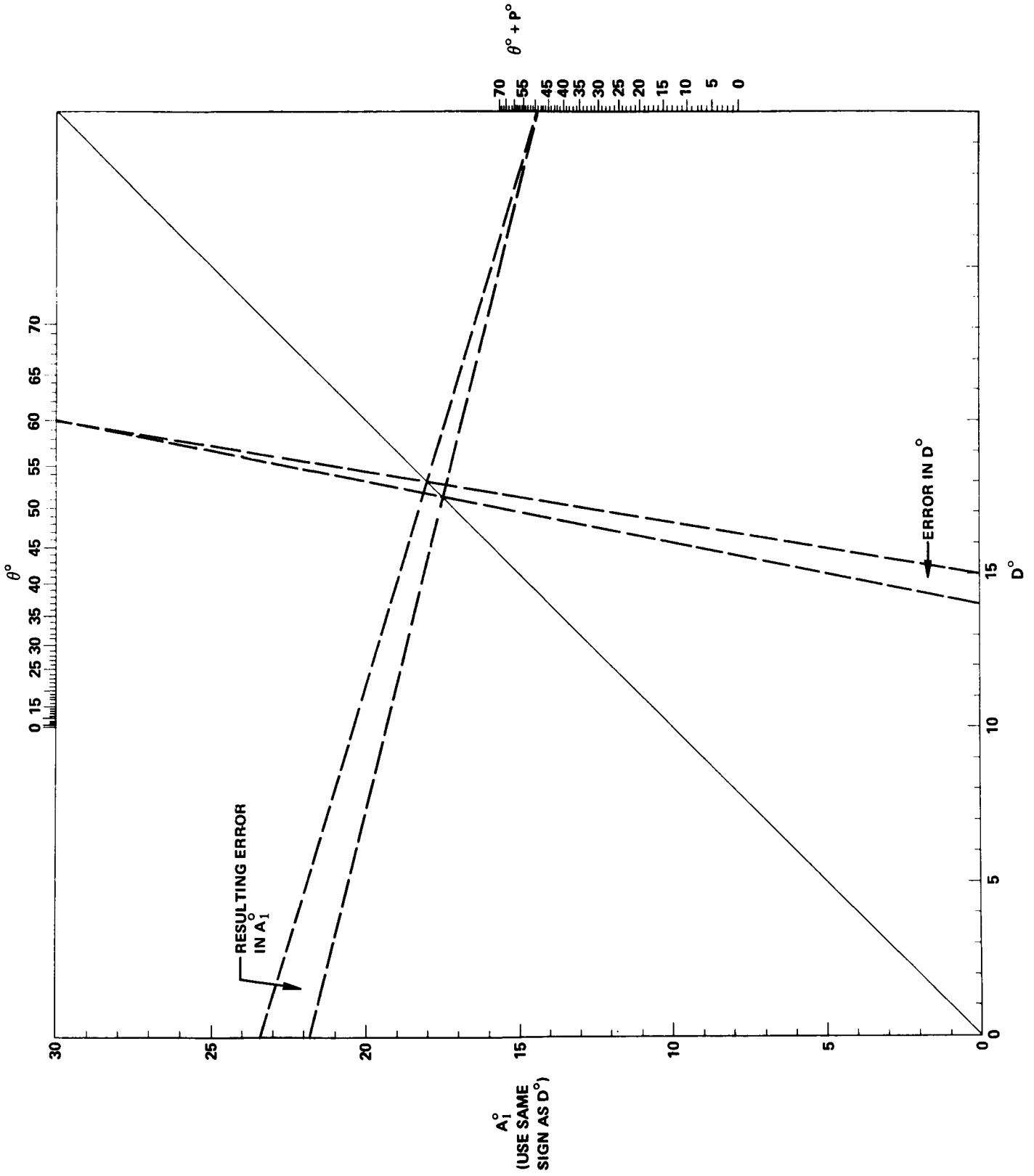


FIGURE 20 - EFFECT OF S. S. D. SCALE READING ERROR

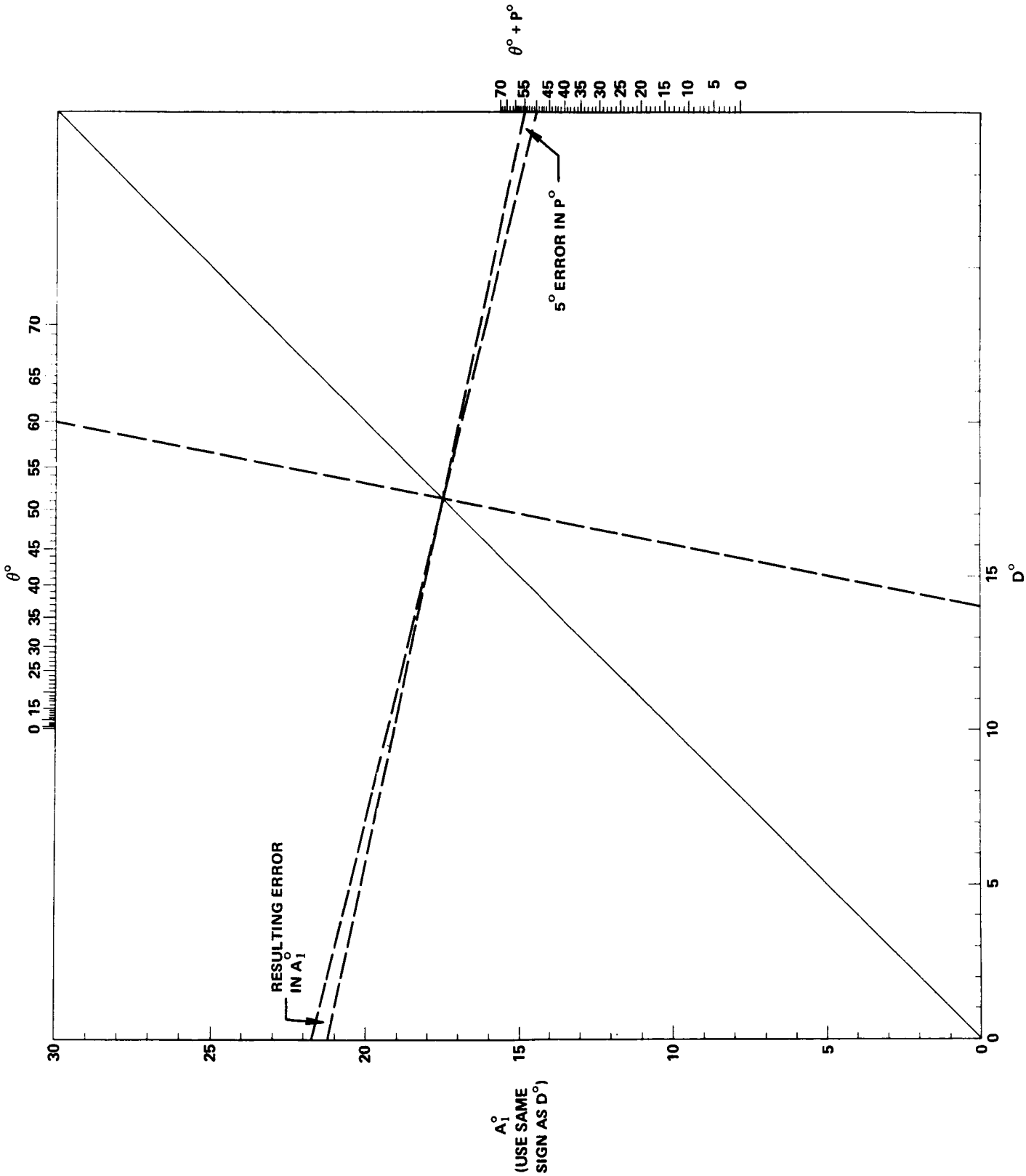


FIGURE 21 - EFFECT OF PITCH READING ERROR

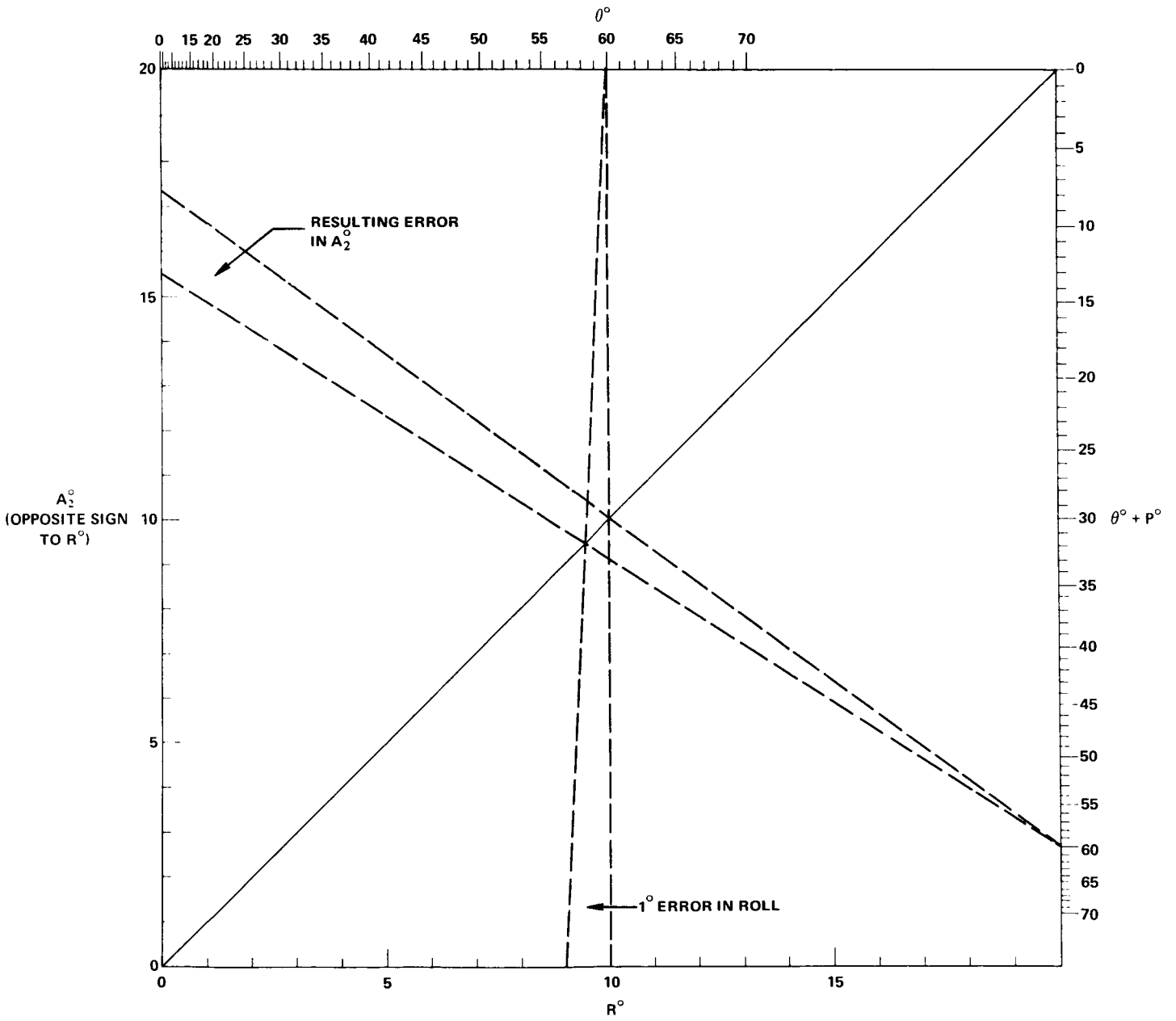


FIGURE 22 - EFFECT OF ROLL READING ERROR

7.0 SUMMARY AND CONCLUSION

The need for the LRV navigation system to establish where science activity occurs and to assist the crew in returning to the LM has been considered. Alternatives, such as navigation using landmarks, craters and other prominent features plus the ability to actually see the LM at a reasonable distance, appear entirely sufficient. Therefore the navigation system should be considered only as a convenience item.

Accuracy requirements for such use which can be achieved with little inconvenience to the crew have been suggested and are compatible with procurement specifications. Operation of the system and effects of errors have been analyzed and discussed. Nomographs useful in aligning the directional gyro have been presented.

Specific conclusions include:

1. Mission rules should not make the LRV navigation system mandatory either to begin or continue a sortie.
2. An accuracy of some 700 m in position at the end of a sortie appears adequate, as do directional gyro drift rates of 10 deg/hour, with alignment accuracy of 3°, using three realignments per sortie.
3. The Sun Shadow Device is not an accurate sundial. Nomographs such as those presented in this memorandum are required, or else a computer routine (also presented). Sun azimuth and elevation variations during a sortie should not be neglected. Changes in directional gyro angle due to LRV pitch and roll should not be neglected when realigning it.
4. The crew should be cautioned to treat the Sun Shadow Device bracket and gnomon carefully. Its accurate alignment is important to S.S.D. accuracy. It may be desirable to review the design of the bracket and gnomon to insure they are strong enough to resist damage.
5. The crew should attempt to read the S.S.D. scale and the LRV pitch and roll angles to within 1° accuracy. The center of the gnomon (tolerance ±0.2") should be used to cast the shadow on the scale.

8.0 ACKNOWLEDGMENTS

Miss G. M. Cauwels efficiently programmed the computer in this study.

Personnel at the Boeing Company gave full and patient cooperation to the authors, which is greatly appreciated.



W. G. Heffron



F. LaPiana

2014-WGH-FL-ksc

BELLCOMM. INC.

REFERENCES

1. J. E. Volder, "The Cordic Trigometric Computing Technique", IRE Transactions on Electronic Computers, September, 1969.
2. Trip Report, "Discussion of LRV Navigation System at Boeing, Seattle", B70 04067, Bellcomm, Inc., I. Y. Bar-Itzhack and F. LaPiana, April 27, 1970.
3. LRV CDR Chart #33, Navigation Subsystem, L. J. McMurtry, (The Boeing Co.), June 16, 1970.
4. Technical Report, "A Compendium of the Moon's Motion and Geometry: 1966 through 1985", TR-68-310-1, Bellcomm, Inc., J. O. Cappellari, Jr., January 9, 1968.
5. A. S. Levens, "Nomography", John Wiley and Sons, Inc., 1959.